Systematic and Applied Microbiology 37 (2014) 68–78

Contents lists available at ScienceDirect

Systematic and Applied Microbiology

journal homepage: www.elsevier.de/syapm

Spatial and temporal variability among marine *Bacteroidetes* populations in the NW Mediterranean Sea

Cristina Díez-Vives, Josep M. Gasol, Silvia G. Acinas*

Departament de Biologia Marina i Oceanografia, Institut de Ciències del Mar, Consejo Superior de Investigaciones Científicas (CSIC), ES-08003 Barcelona, Catalunya, Spain

ARTICLE INFO

Article history:
Received 14 May 2013
Received in revised form 25 July 2013
Accepted 21 August 2013

Keywords:
Bacteroidetes populations
Diversity
Structure
DGGE
CARD-FISH
Spatial and temporal variability

ABSTRACT

The abundance and structure of *Bacteroidetes* populations at diverse temporal and spatial scales were investigated in the Northwestern Mediterranean Sea. At a temporal scale, their relative abundance exhibited a marked seasonality, since it was higher in spring and decreased in winter. Similarly, *Bacteroidetes* community structure encompassed three main groups (winter, spring and summer-fall), which mimicked global bacterioplankton seasonality. At the spatial scale, relative abundances were similar in all surface samples along an inshore–offshore transect, but they decreased with depth. Analysis of the community structure identified four markedly different groups mostly related to different depths. Interestingly, seasonal changes in abundance and community structure were not synchronized. Furthermore, richness was higher when *Bacteroidetes* were less abundant. The variability of *Bacteroidetes* contributions to community structure in the temporal and spatial scales was correlated with different environmental factors: day length was the most important factor at the temporal scale, and salinity at the spatial scale. The community composition in terms of phylotypes changed significantly over time and along the depth gradients, but season or depth-specific phylogenetic clusters were not identified. Delineation of coherent *Bacteroidetes* sub-clusters should help to uncover higher resolution patterns within *Bacteroidetes*, and explore associations with environmental and biological variables.

Introduction

Members of the phylum *Bacteroidetes* are particularly common in the oceans, representing in some sites up to 40% of total bacteria counts determined by in situ hybridization [4,18,40,47]. *Bacteroidetes* often constitute the most abundant bacterial group in polar marine environments [48,75,82] and coastal waters [18,19,28,60], as well as in upwelling systems [72], particularly during phytoplankton blooms [1,3,28,56,64,75], indicating a certain preference for productive habitats. Their ability to degrade polysaccharides and proteins [19,34,47] suggests that they may play a key role as consumers of algae-derived metabolites. Some studies have also suggested that they occupy a "particle-specialist" niche [21,22,24]. However, others have reported their presence in both attached and free-living niches, with some differences between the populations occurring in both fractions [21,32,69].

Several studies have focused on the quantification of total marine *Bacteroidetes* (e.g. [4,33]), and some have differentiated distinct *Flavobacteria* clusters [15,28,41,48,54,79]. In addition, a few group-specific fingerprinting studies have described the dominant populations in a variety of habitats [25,45,67,70,69]. However, comprehensive studies of specific populations at spatial and temporal scales are largely unexplored (e.g. [14]).

Some data on *Bacteroidetes* community dynamics have been derived from the study of bacterioplankton communities using DGGE with universal primers, but these have usually recovered few *Bacteroidetes* bands (e.g. [4,16,46,69,74]), or even none (e.g. [68]). In addition, biases of universal bacterial primers against *Bacteroidetes* have been widely reported [18,27,48]. Group-specific primers are likely to provide a more detailed view of specific groups (e.g. [69]), but even group-specific oligonucleotide probes, such as the highly used CF319a, may not yield accurate quantitative data [1,9] due to limited group coverage and specificity [25].

In this study, *Bacteroidetes* dynamics and structure were explored at temporal and spatial scales, analyzing the influence of environmental and biological factors on the abundance and composition of this group. The study focused on the Northwestern Mediterranean Sea, with monthly sampling during a 2-year time series along a spatial transect that included five stations with vertical profiles covering the main hydrographical features of the inshore–offshore gradient.

* Corresponding author. Tel.: +34 93 230 8565; fax: +34 93 230 95 55.
E-mail address: sacinas@icm.csic.es (S.G. Acinas).

0723-2020/$ – see front matter © 2013 Elsevier GmbH. All rights reserved.
http://dx.doi.org/10.1016/j.syapm.2013.08.006

Materials and methods

Sampling

The seasonal study was conducted at the Blanes Bay Microbial Observatory (BBMO, http:\\www.icm.csic.es/bio/projects/icmicrobis/bbmo/) (41°40′ N, 2°48′ E), from September 2006 to September 2008. This site is relatively oligotrophic [37], and only 1 km offshore. Surface (0.5 m depth) waters were sampled monthly, filtered through a 200 μm mesh net and transported to the laboratory (within 1.5 h) under dim light in 25 L polycarbonate carboys.

Vertical profile samplings were also carried out at five stations along an inshore–offshore transect (Fig. S1). This transect was sampled from on board the "BO García del Cid" during the "Modivus" cruise (September 20–23, 2007). The area has been repeatedly studied for physical oceanography [72], water chemistry [26], phytoplankton [30,29,31], bacteria [36,61,65], or viruses [43]. Samples were collected with Niskin bottles mounted on a rosette equipped with a SAIV A/S model SD204 CTD. Water was prefiltered through a 200 μm mesh and processed immediately on board.

Environmental and biological variables

Methods for measurements of water temperature, chlorophyll a (Chl *a*) concentration, fluorescence, and dissolved inorganic nutrient concentrations were standard, and have been previously described (e.g. [7]). *Synechococcus*, *Prochlorococcus* and photosynthetic picoeukaryotes were enumerated by flow cytometry and distinguished by their different sizes and pigment properties in unstained samples following common procedures (i.e. [55]). Heterotrophic prokaryotes were also counted by flow cytometry [35] after staining with SybrGreen I. Chl *a* concentration and photosynthetic picoplankton were not measured at depths below 140 m.

Catalyzed reporter deposition-fluorescence in situ hybridization (CARD-FISH)

For determination of *Bacteroidetes* abundance by CARD-FISH [62], 25 mL seawater samples were fixed with 2% paraformaldehyde (final concentration) overnight at 4 °C in the dark, and gently filtered through 0.2 μm polycarbonate filters (OSMONICS INC., 47 mm), which were rinsed with Milli-Q water and stored at −20 °C until processing. The labeling procedure was carried out using a *Bacteroidetes*-specific oligonucleotide probe CF968 (5′-GGTAAGGTTCCTCGCGTA-3′). This probe has been previously published as a PCR and QPCR primer [17,23]. In a recent revision, coverage of CF968 for the phylum *Bacteroidetes* was 92.8%, with a high specificity [25]. Recently, the probe has been successfully applied in the CARD-FISH protocol (Acinas et al., unpublished). Briefly, CF968 was synthesized with a 5′-aminolink (Thermo Fischer Scientific Ulm, Germany) and subsequently labeled with HRP (Roche Diagnostics, Barcelona, Spain) according to Urdea et al. [80] and Amman and Fuchs [9]. The optimal formamide concentration for the CF968 probe was found to be 55% (Acinas et al., unpublished). Counts were obtained from a minimum of 18 microscope fields representing more than 1000 DAPI-positive cells on each filter. The results (mean and standard deviation) were expressed as the percentage of positive CARD-FISH cells relative to the total DAPI-stained cells (Table S1).

DNA extraction and PCR-DGGE

To collect bacterioplankton biomass, seawater (8–10 L per sample) was filtered sequentially using a peristaltic pump through GF/A filters (47 mm, Whatman) and polycarbonate 0.22 μm pore size filters in the spatial study (Modivus). For samples taken at the coastal surface station (BBMO), 47 mm diameter, 3 μm pore polycarbonate filters (Whatman) and 0.22 μm pore Sterivex filters (Durapore, Millipore) were used. The Sterivex units were treated with 1.8 mL lysis buffer (50 mM Tris–HCl, 40 mM EDTA, 0.75 M sucrose, pH 8.0) and kept at −80 °C, whereas the Modivus filters were stored directly at −80 °C after flash freezing in liquid N_2. Microbial biomass was digested with lysozyme, proteinase K and sodium dodecyl sulfate, and the nucleic acids were extracted with phenol and concentrated in a Centricon-100 (Millipore), as described in Massana et al. [57].

DNA samples were amplified for DGGE analyses using a *Bacteroidetes*-specific forward primer (GC-CF418) with a universal bacterial reverse primer (907RM), as described previously [25]. In order to compare *Bacteroidetes* with bacterioplankton community fingerprints, additional DGGE analyses were carried out with samples from a 1-year time series (from September 2007 to September 2008) using universal bacterial primers (GC-358F and 907RM) [59] under similar PCR conditions. In both cases, the forward primer included a 5′-CG-clamp (CGC CCG CCG CGC GCG GCG GGC GGG GCG GGG GCA CGG GGG G). Optimization of the template DNA amount (1 ng, 4 ng, 8 ng and 10 ng DNA per reaction) was necessary in order to improve PCR yields with environmental samples, depending on the levels of inhibitory residues present. PCR reactions (50 μL final volume) contained 200 μM of each deoxynucleoside triphosphate, 0.2 μM of each primer, 2 mM $MgCl_2$, 1× PCR buffer, and 1 U Taq DNA polymerase (Invitrogen). The amplification cycle consisted of an initial denaturation step (94 °C, 5 min); 30 cycles of denaturation (94 °C, 30 s), annealing (55–63 °C, 30 s), and extension (72 °C, 1 min); and a final extension (72 °C, 10 min). PCR products were analyzed and quantified by agarose gel electrophoresis using standards (Low DNA Mass Ladder, GIBCO BRL). To mitigate random biases associated with individual reactions, three PCRs of the same template were run and pooled prior to the DGGE analyses. Similar amounts of the PCR products were loaded on 6% polyacrylamide gels cast in a continuous DNA-denaturing gradient (40–70% for *Bacteroidetes*-specific and 40–80% for universal bacterial gels; 100% denaturant was 7 M urea in 40% deionized formamide). Gels were run at 100 V for 16 h at 60 °C in TAE running buffer (40 mM Tris pH 7.4, 20 mM sodium acetate, 1 mM EDTA) using a DGGE-2000 system (CBS Scientific, Del Mar, CA, USA). The gels were stained with SYBR Gold (Molecular Probes, Eugene, OR, USA) for 15 min and documented with a Fluor-S MultiImager system (Bio-Rad, Hercules, CA, USA).

Relative quantification of DGGE fingerprints

Gel images were analyzed using the Quantity-One software (Bio-Rad). The bands occupying the same position in different lanes of the gels were identified and refined by visual inspection. A data matrix was constructed considering the presence or absence of individual bands in each lane and their relative percentage contribution to the total absorbance of the lane. This dataset was analyzed using the software PRIMER 6 (Primer-E Ltd.). A distance matrix was calculated using the Bray–Curtis dissimilarity, and a dendrogram was obtained from the resemblance matrix by the unweighted pair-group method with arithmetic mean (UPGMA). "Similarity profile" (SIMPROF) permutation tests were computed over the dendrograms, seeking statistically significant evidence for the existence of genuine clusters in samples that were a priori unstructured. These tests were undertaken at each node in order to verify whether the subgroups had significant internal structure. The distance matrix was also used for a similarity analysis by one-way ANOSIM with all possible permutations.

Table 1
Spearman rank correlations between environmental factors and *Bacteroidetes* percentage contribution to the bacterial community. Statistically significant correlations, $p < 0.01$ (**) or $p < 0.05$ (*), are highlighted in bold. $N = 25$ for the temporal series and $N = 17$ for the spatial transect.

		Temporal		Spatial	
		r_s value	p value	r_s value	p value
Physical	Depth	n.a.	n.a.	−0.388	0.124
	Temperature	0.053	0.801	**0.560****	**0.019**
	Fluorescence	n.a	n.a	−0.047	0.857
	Day length	**0.444****	**0.026**	n.a.	n.a.
	Oxygen	n.a.	n.a.	0.161	0.538
	Salinity	−0.326	0.112	**−0.609****	**0.009**
	PO_4	0.185	0.477	−0.166	0.524
	NH_4	**−0.499**	**0.011**	−0.053	0.839
	NO_2	−0.017	0.936	−0.095	0.716
	NO_3	0.252	0.225	−0.451	0.069
	SiO_4	−0.083	0.693	**−0.589***	**0.013**
Biological	Chl *a*	0.044	0.833	0.087	0.740
	Chl *a* < 3 μm	−0.006	0.977	0.064	0.808
	Prochlorococcus	**−0.525****	**0.007**	0.195	0.453
	Synechococcus	−0.055	0.793	0.216	0.405
	Photosynthetic picoeukaryotes	−0.105	0.619	0.294	0.251
	Bacteria	**−0.442***	**0.027**	0.137	0.599

Sequencing and phylogenetic analysis

The DGGE bands were excised, placed in 20 μL Milli-Q water, and incubated overnight at 4 °C. The supernatants (2 μL) were used as template DNA for re-amplification with the original primer set (without the GC-clamp) and the products were submitted for automated Sanger sequencing (Macrogen Inc., Amsterdam, Netherlands). Several bands occupying the same position in different gel lanes were excised and sequenced to confirm correct matching of the bands. Due to the large number of bands per lane and their proximity in the universal bacteria DGGE, the excised bands were re-amplified and re-run into a new DGGE to verify their position and uniqueness.

The sequences obtained from the DGGE bands were compared against GenBank, National Center for Biotechnology Information (http://www.ncbi.nlm.nih.gov/) using BLAST [8] to determine their phylogenetic affiliation. Sequences were aligned with homologous 16S rRNA sequences from the SILVA SSU Reference NR database release 106, using the automated aligning tool contained in the ARB software package (http://www.arb-home.de) [52]. The aligned sequences were added to the guide tree using the "*quick add*" parsimony tool, which does not alter the starting tree topology. The resulting tree was pruned to retain only the relevant closest taxa. Average pairwise percentage similarity of overall 16S rDNA sequences, as well as average similarity within and between groups was estimated from an alignment of 54 *Bacteroidetes* sequences using the MEGA5 program [78]. Gene sequences were deposited in GenBank under accession numbers JX865538–JX865592.

Statistics

Two different statistical analyses were performed. Firstly, in order to explore the pairwise correlations globally using raw values, Spearman's rank correlation tests were performed between the *Bacteroidetes* relative contribution to the total abundance of Bacteria (referred to as the *Bacteroidetes* percentage throughout the paper) and the biological and environmental variables included in Table 1. Correlations were analyzed for significance ($p < 0.05$ or $p < 0.01$) by a Student's 2-tailed *t*-test. Secondly, multiple regression analyses were carried out with the *Bacteroidetes* percentage as the dependent variable and the biological/environmental variables as predictors. This allowed the combination of the variables that explained most of the variability of the *Bacteroidetes* percentage observed to be determined. Forward stepwise multiple regression was used where the independent variables were individually added to the model at each step of the regression until the "best" regression model was obtained. The variable entered at each step was the one that produced the largest increase in R^2 (i.e. the one with the largest Pearson's partial correlation with the *Bacteroidetes* percentage). This procedure tests the significance of all the variables in the model, and those that are not significant are excluded before the next forward selection step (only intercepts and variables with significant ($p < 0.05$) contributions to the regression model are retained) [76]. Multicollinearity was tested for between the predictor variables. This enabled the correlations between predictor variables to be explored, and the tolerances for each variable to be calculated [76]. Statistical analyses were performed using SPSS v.19.0.

Results

Temporal dynamics in BBMO

The BBMO site was characterized by a clear seasonality (Fig. S2A), with temperature values ranging from 12.9 to 26.2 °C and salinity from 37 to 39 psu. Summers were characterized by high water temperature (20–26 °C), and low concentration of inorganic nutrients (e.g. $PO_4 = 0.1$ μM) and Chl *a* (ca. 0.3 μg L^{-1}). In contrast, winters showed water temperatures of 13–16 °C and a higher concentration of nutrients (e.g. $PO_4 = 1.1$ μM) and Chl *a* (1–2 μg L^{-1}). December 2006 and January 2007 displayed slightly warmer temperatures than the following year. Bacterial abundance values were quite stable ranging between 0.43 and 1.6×10^6 cells mL^{-1}. *Synechococcus* abundance was typically high in summer and contributed up to 13.8% of total prokaryote numbers. *Prochlorococcus* values were usually lower (up to 4.5%) and increased in the fall and winter, when *Synechococcus* started to decline. Photosynthetic picoeukaryotes were more abundant during late winter and spring (up to 1.7×10^4 cells mL^{-1}), and declined during the summer (details not shown).

Abundance of Bacteroidetes and their environmental and biological predictors. The abundance of *Bacteroidetes* was quantified by CARD-FISH during the 2-year time series at the BBMO station. The percentage contribution of *Bacteroidetes* to the total community was variable over time and accounted for 8–22% of total DAPI counts (Table S1). A seasonal pattern was observed, with the highest values measured from April to May in 2007 and from April to August in 2008, with a marked descent after these periods (Fig. 1A).

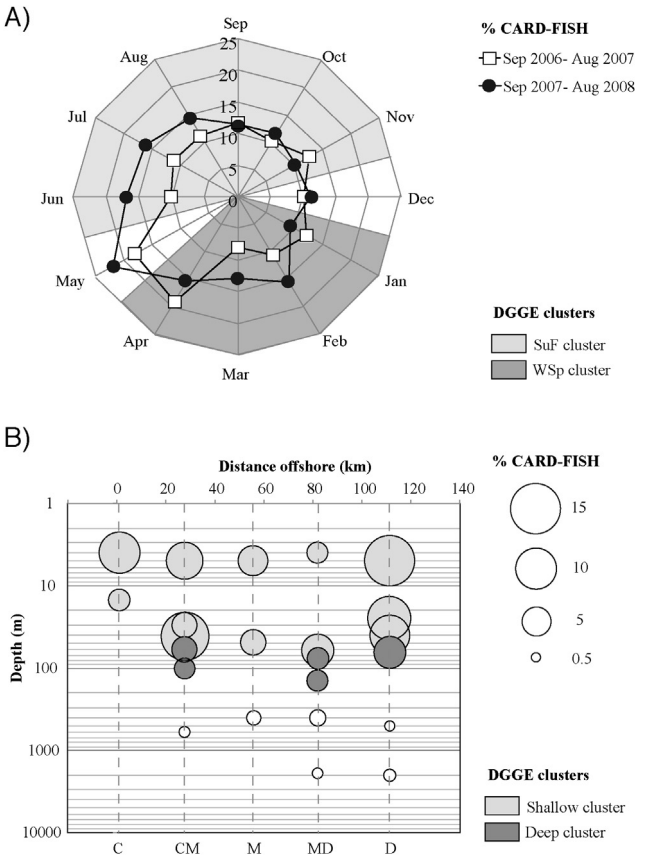

Fig. 1. Percentage of *Bacteroidetes* in CARD-FISH counts: (A) over two consecutive years in the temporal study, represented as circles and squares, and (B) in the spatial study, represented as circle areas for each sample point. The groups defined by the DGGE clustering analyses (SuF/WSp or Shallow/Deep) are also represented as different gray tones. Since transitional months (May and December) fell into different clusters in the 2 years analyzed they are colored in white. Samples less than 200 m (not included in the DGGEs) are also in white.

In terms of absolute abundances, *Bacteroidetes* counts were significantly higher ($p < 0.001$, ANOVA $F(1, 23) = 24.94$) from April to August ($10.0 \pm 1.0 \times 10^4$ cells mL^{-1}) than from September to March ($7.8 \pm 1.5 \times 10^4$ cells mL^{-1}) in both years (Table S1).

In the bivariate correlation analyses, only two physical and two biological variables showed a significant correlation with the *Bacteroidetes* percentage in the temporal series: positive with day length and negative with ammonia, *Prochlorococcus* and total bacteria abundance (Table 1). Multiple regression analyses of the temporal series explained a relatively large fraction of the variability of the *Bacteroidetes* percentage contribution to community structure with only a few environmental/biological variables. The best model explained 57.5% of the variability of the *Bacteroidetes* percentage with only three variables in the following order and sign: day length (+), total bacterial abundance (−) and NH_4 (−) (see Table 2 for the cumulative R^2 explained by each variable). This model did not include *Prochlorococcus* counts, which was the variable with the largest Spearman's rank correlation value. There was no correlation between the predictor variables and, hence, no collinearity test was needed. The model residuals were further tested and they were normally distributed, as required by this procedure. The same multiple regression analyses were also performed using *Bacteroidetes* abundance and similar results (Table S2) were obtained.

Community composition by DGGE analyses. The temporal dynamics were analyzed from September 2006 to September 2008, using DGGE fingerprinting with *Bacteroidetes*-specific primers. Samples from November 2006, as well as June and July 2008, did not yield enough PCR product to be included in the dataset. Image analyses of the 22 remaining samples resulted in 292 bands identified in 31 unique positions (Fig. S3). The number of bands per sample was between 6 and 17. In general, 50% of the bands accounted for more than 80% of the total intensity per lane. No band appeared consistently in all samples throughout the year. In the clustering analyses, samples were classified in two main groups that had a 35% similarity: "Winter-Spring" (WSp) and "Summer-Fall" (SuF) (Fig. 2). More bands were observed in the WSp group (mean = 15.6, $n = 10$) than in the SuF group (mean = 11.3, $n = 12$) ($p < 0.001$, ANOVA $F(1, 20) = 16.68$). The band pattern shifted significantly in the transition from winter to spring (Fig. S3). However, from the early summer to fall, the fingerprint pattern was relatively stable. Within the WSp group, two subgroups could be distinguished during this period at a similarity of 47%: early and late. Likewise, within the SuF group, samples taken at the end of the period clustered apart from earlier samplings, although these groups were not significantly different (Fig. 2). ANOSIM tests significantly supported the existence of three groups in this seasonal series (T1, T2 and T3 in Fig. 2) (Global $R = 0.824$, one-way ANOSIM $p < 0.001$).

In order to test whether the dominant bacterioplankton populations mirrored this seasonal clustering observed among *Bacteroidetes*, a 1-year time series (September 2007–September 2008) was analyzed by DGGE using universal bacterial primers (Fig. S5A) and it was compared to the *Bacteroidetes*-specific DGGE from the same dates (Fig. 2). The analysis of the universal bacteria gel yielded a total of 420 detectable bands in 61 different positions among the 13 samples analyzed. The number of bands per sample was rather stable varying between 30 and 35. Minor differences were observed between the bacterial (Fig. S5B) and the *Bacteroidetes*-specific dendrograms (Fig. 2), such as in the Dec07 and Jan08 samples, which branched off from other winter samples. Samples Jun08 and Jul08 were not present in the *Bacteroidetes* dendrogram and their position could not be compared within the clustering.

Spatial transect

The spatial sampling (September 2007) included stations along a transect from coastal waters to open ocean stations above a maximal water column of 2500 m (Fig. S1). At the time of sampling, the surface water temperature was 23–24 °C from coast to offshore while it dropped to under 14 °C below 100 m (Fig. S2B). The thermocline was located between depths of 30 and 40 m at stations CM, M and D, whereas station MD had a superficial temperature drop (from 22 to 19 °C in the first 10 m) and a second temperature drop at 60 m (from 18 to 14 °C). This was caused by a small cyclonic gyre (details not shown) that upwelled colder, deep water. Maximum values of Chl *a* were found between 60 and 80 m (Fig. S2B). A Chl *a* peak of up to 1.15 μg L^{-1} was present in the DCM layer at 44 m in station CM (mostly associated with >3 μm particles, i.e. nano- and microphytoplankton). *Synechococcus* presented maximal abundance inshore and at upper water layers (above 27 m), whereas *Prochlorococcus* peaked offshore and at deeper layers (50 m). Phototrophic picoeukaryotes values reached 7.87×10^3 cells mL^{-1} at 44 meters in station CM (details not shown).

Spatial patterns of Bacteroidetes abundance and their environmental and biological predictors. In the spatial transects, the maximal abundance of *Bacteroidetes* was usually observed in surface waters (5 m) (average 9.6% of DAPI counts or $5.2 \pm 2.3 \times 10^4$ cells mL^{-1}), with the exception of station MD (at the upwelling core), where they represented only 2.6% of the DAPI counts (Table S1). In general, the contribution of *Bacteroidetes* decreased with depth (Fig. 1B), although high relative values were detected at 44 m in station CM, reaching up to 13.7% (1.35×10^5 cells mL^{-1}) and matching the

Table 2
Summary of multiple regression models (forward procedure) for the temporal series and the spatial transect. The independent contributions of each variable to the prediction of *Bacteroidetes* percentages after controlling for all other independent variables are shown (β, or standardized regression coefficients). *P* values are the significance of each predictor variable within the model. R^2 corresponds to corrected variance explanation.

Dependent variable	Predictor variables	Cumulative R^2	β	p
Bacteroidetes percentage (temporal series)	Day length	0.218	0.627	0.000
	Bacteria	0.467	−0.514	0.002
	NH_4	0.575	−0.342	0.021
Bacteroidetes percentage (spatial transects)	Salinity	0.436	−0.944	0.000
	Synechococcus	0.653	−0.538	0.002
	Picoeukaryotes	0.786	0.363	0.008

aforementioned Chl *a* peak at this station (1.15 μg Chl $a\,L^{-1}$) (Fig. S2).

Bivariate correlations between the *Bacteroidetes* percentage, and the environmental and biological variables for the spatial transect (in samples above 140 m), indicated a positive correlation with temperature and a negative correlation with salinity and SiO_4 (Table 1). The best model derived from multiple regression analyses for the spatial transect explained 78.6% of the *Bacteroidetes* percentage with three variables: salinity (−) and *Synechococcus* abundance (−), and picoeukaryote concentration (+) (Table 2). Collinearity was tested for between salinity and *Synechococcus* because they were correlated ($r = -0.762$, $p < 0.001$). These two predictor variables explained a different proportion of the *Bacteroidetes* percentage (Table 2) and, since the tolerance value was relatively high (0.708), multicollinearity was rejected. Again, model residuals were normally distributed. Multiple regression analyses using *Bacteroidetes* abundance gave almost identical results (Table S2).

Community composition by DGGE analyses. DGGE fingerprinting was carried out for the spatial transect samples using the *Bacteroidetes*-specific primers. Due to the weak amplification of samples below a depth of 400 m, downstream analyses could not be carried out, although *Bacteroidetes* were detected by CARD-FISH down to 2000 m (Table S1). The gel displayed 211 detectable bands in 47 positions (Fig. S4). The number of bands per sample was rather variable, ranging between 7 and 20. No band appeared consistently in all samples, and only 10 bands were present in at least half of the samples. Changes in *Bacteroidetes* composition were mostly associated with depth rather than with the horizontal gradient (i.e. distance from shore). Two main groups were detected with less than 20% similarity between them (Fig. 3). The "Deep" group showed a higher number of bands (mean = 16.8, $n = 5$) than the "Shallow" group (mean = 11.5, $n = 10$) (ANOVA $p = 0.03$, $F(1,13) = 13.94$). Sample CM44 presented a rather unique profile, clustering loosely to "Shallow" samples (40% similarity). Within these two groups, samples above 30 m (i.e. above the thermocline as defined before) clustered apart from those collected below the thermocline. In the "Deep" group, samples collected in the DCM (between 60 and 80 m) clustered separately from those sampled below this region (CM100, MD140) (Fig. 3). These four groups (S1–S4) were significantly different (Global $R = 0.930$, one-way ANOSIM $p < 0.001$).

Sequencing and relative abundance of marine Bacteroidetes phylotypes

In both *Bacteroidetes*-specific gels (spatial transects and temporal series), the 55 predominant bands were excised and successfully sequenced (300–450 pb). A total of 23 sequences were obtained from bands of the temporal analysis gels and 32 sequences from the spatial ones. Several bands occupying the same position in the gels were excised from different lanes and sequenced to confirm the matching analysis. Most of the DGGE signal could be sequenced, since these bands accounted for roughly 80% of the average intensity per lane. All the sequences obtained from both the temporal and spatial studies were related to the phylum *Bacteroidetes*, except for one identified as phylum *Verrucomicrobia* (BBMO-59) (Tables S3 and S4). In the phylogenetic analyses, four sequences belonged to class *Sphingobacteria* and the remaining 51

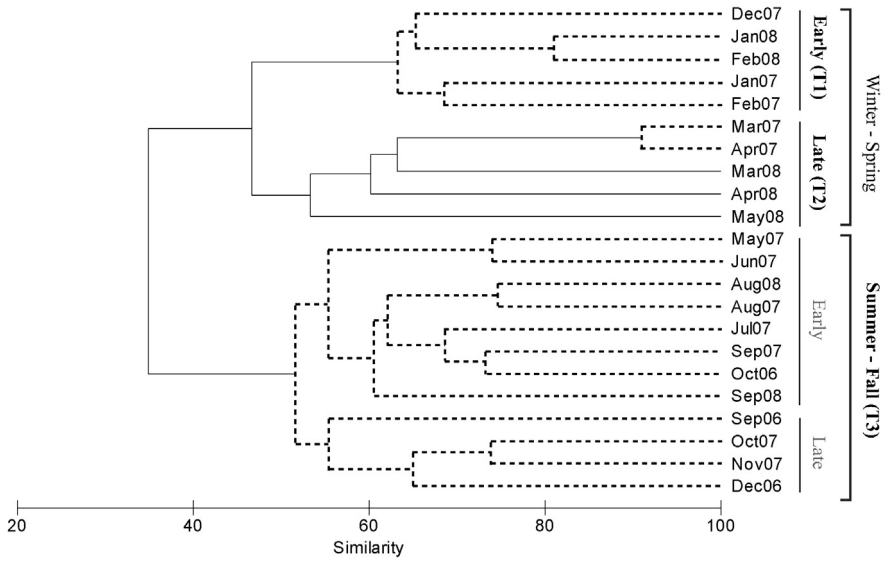

Fig. 2. Cluster analyses of *Bacteroidetes* DGGE banding patterns using UPGMA. (W) Winter, (Sp) Spring, (S) Summer, (F) Fall. T1, T2 and T3 represent significantly different clusters in the seasonal series. The Distance matrix was calculated using the Bray–Curtis similarity algorithm. (Branches marked with dotted lines indicate that the SIMPROF analysis could not find statistical evidence for any sub-structure within these clusters.)

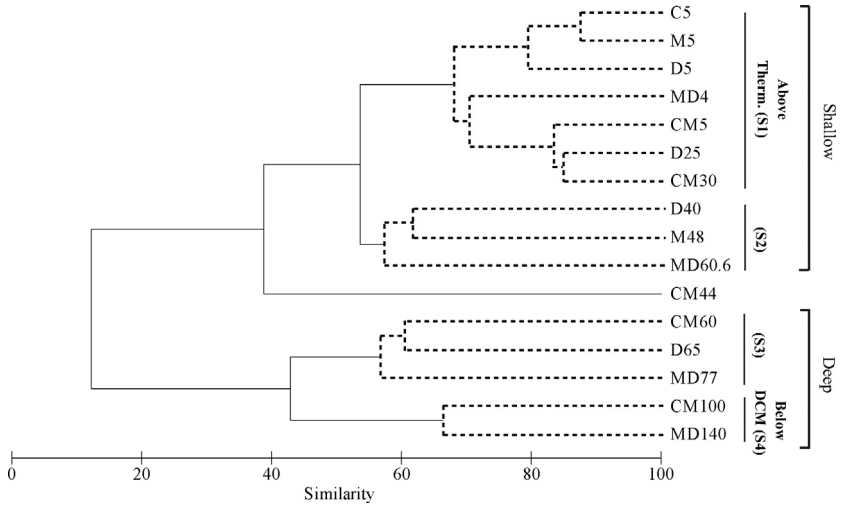

Fig. 3. Cluster analyses of *Bacteroidetes* DGGE banding patterns using UPGMA. Therm., thermocline; DCM, deep chlorophyll maximum. S1, S2, S3 and S4 represent significantly different clusters in the spatial samples. The distance matrix was calculated using the Bray–Curtis similarity algorithm. (Branches marked with dotted lines indicate that the SIMPROF analysis could not find statistical evidence for any sub-structure within these clusters.)

to class *Flavobacteria*. The *Sphingobacteria* sequences were related to the family *Saprospiraceae* and they were recovered exclusively in the temporal series study during spring and summer. These were present at the lowermost end of the gels (Fig. S3). The *Flavobacteria* sequences grouped into two families: *Flavobacteriaceae* and *Cryomorphaceae*. Fourteen of them grouped with clusters that included cultured representatives (*Fluviicola*, *Owenweeksia*, *Polaribacter* and *Tenacibaculum*) (see Fig. 6) while the remaining were assigned to uncultured isolates, mainly to North Sea clusters (as characterized by Alonso et al. [4]).

In order to explore the contribution of different *Bacteroidetes* phylotypes throughout the temporal and spatial scales, the relative intensity of the bands in the DGGE analyses was measured. During the 2-year time series, this relative intensity of bands corresponding to specific phylotypes changed gradually over the seasons. A representation of these patterns (limited to the sequenced bands) is shown in Fig. 4. Some phylotypes (e.g. BBMO-4, -5, -15, -25, -29, -32, -37, -49, -54) were mostly present in "WSp" months whereas others were dominant in the "SuF" group (e.g. BBMO-14, -19, -22, -35, -52, -56). These season-specific phylotypes were recurrent over the 2 years analyzed (Fig. 4). A remarkable pattern shift between these communities was noticed between April and May 2007 together with an increase in the intensity of another three phylotypes (BBMO-50, -51, -55) only during the transition (Fig. 4). A similar pattern shift was detected between October and November 2007. The same shifts were expected to occur from SuF to WSp in 2006 and WSp to SuF in 2008 but, unfortunately, these samples did not amplify. Only one phylotype (BBMO-46) was abundant throughout both years.

The BBMO station and station C that were close to each other were also compared and, although only seven sequences were retrieved from C5, at least one of them (MOD_Sep_M5F_18,) clustered with the BBMO coastal site.

A clear shift in the *Bacteroidetes* communities was observed along the spatial gradient from the surface to deep waters (Fig. 5). Samples from moderate depths (i.e. 40–70 m) typically presented transitional patterns in which both "Shallow" and "Deep" bands could be detected (Fig. 5).

According to the sequence data analysis, the *Bacteroidetes* sequences had an average pairwise percentage similarity of 90.9%

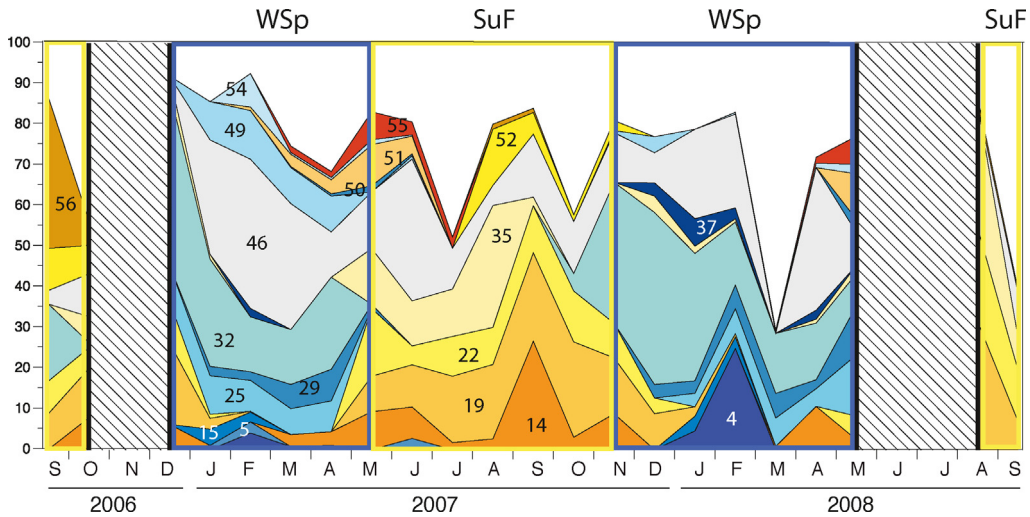

Fig. 4. Relative intensity of the sequenced DGGE bands during the 2-year time series. Colored blocks split the samples into WSp (blue) or SuF (yellow) groups according to the clustering obtained in the DGGE profile analyses. Then, the relative intensity of the bands is represented using yellow (WSp) or blue (SuF) color palettes. (Nov 06, Jun 08 and Jul 08 were not included in the analyses). The numbers indicate the #ID of the band (Fig. S3 and Table S3).

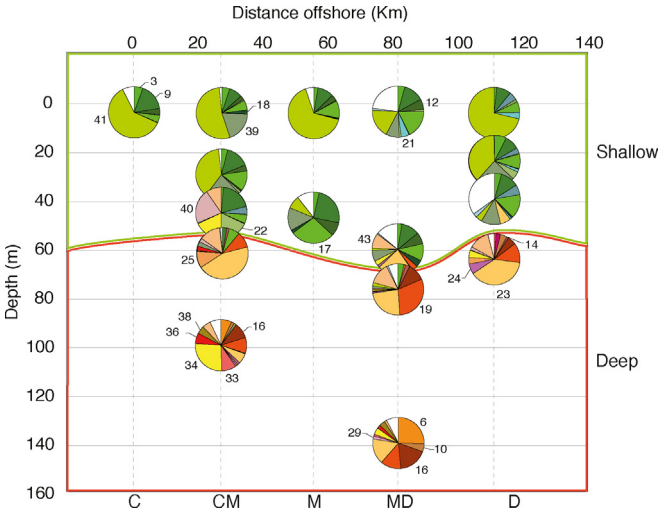

Fig. 5. Relative intensity of the DGGE bands sequenced from the horizontal and vertical profiles in the spatial study (Modivus cruise). Colored blocks split the samples into Shallow (green) or Deep (red) groups according to the clustering obtained in the DGGE profile analyses. The relative intensity of the main bands is represented using green (Shallow cluster) or red (Deep cluster) color palettes. The numbers indicate the #ID of the bands (Fig. S4 and Table S4). (For interpretation of the references to color in this figure legend, the reader is referred to the web version of the article.)

(Table S5). After assigning the sequences to taxonomic groups, mean similarity within each phylogenetic cluster ranged from 93.9 to 99.5%, whereas similarity between clusters only averaged 88.8% (Table S5). In the phylogenetic analysis (Fig. 6), the main phylogenetic clusters included sequences from mixed seasons and depths. For example, the predominant sequences in groups "WSp" (BBMO-29) or "SuF" (BBMO-19, -22, and -25) branched within the NS4 cluster (similarity of the NS4 cluster = 97.5%) (Fig. 6). Similarly, "Shallow" samples (MOD-9, -12, -17, -18, -39a, and -41) and "Deep" samples (MOD-6, -10, -16, and -19) branched in the same NS4 cluster.

Discussion

An oligonucleotide group-specific probe and primers were used to describe the abundance and distribution of *Bacteroidetes*, a key bacterial group in marine environments, across a spatial gradient and through a temporal series. The current study focused on "free-living" communities (fraction 0.22–3 μm). In previous studies, we had analyzed the particulate fraction (3–20 μm) of some of the same samples included here, and similar DGGE patterns and phylotypes were obtained upon sequencing of the bands to those obtained here with the free-living fraction [25] (Fig. 6). This agrees with studies that have found the same phylotypes in different fractions, at least for the most abundant *Bacteroidetes* [1,67,83] (but see [32,69]).

Temporal changes of Bacteroidetes assemblages

It was found that the contribution of *Bacteroidetes* abundance to total bacterioplankton varied between 8 and 22%, a range typically reported in coastal environments. In addition, the percentage contribution values peaked in spring and early summer, which was similar to reports from other marine habitats [3,28,46,56,63]. However, these changes in the abundance of *Bacteroidetes* were not synchronized with changes in their community structure. Thus, it was observed that *Bacteroidetes* abundances usually increased from March to April but a similar community structure remained until May (Fig. 1A). A similar pattern was observed after the abundance drop by the end of the summer (from August to September), maintaining the summer community structure until November when it shifted to the winter pattern.

A substantial temporal variability was found among the 31 *Bacteroidetes* phylotypes characterized in this study (see Fig. 4). The detailed analysis of the *Bacteroidetes* community patterns supported the clustering into two main groups (Winter-Spring, WSp and Summer-Fall, SuF) following a seasonal scheme. Interestingly, the fingerprinting of total bacterioplankton (with universal bacterial primers) also resulted in a similar clustering (Fig. S5B), suggesting that the *Bacteroidetes* seasonal changes paralleled those of the whole bacterial assemblage. Each group of samples (WSp and SuF) was characterized by markedly different communities (i.e. specific phylotypes in each group) that were recurrent for two consecutive years (Fig. 4). However, these distinct phylotypes were not distantly phylogenetically grouped as they grouped together in the same phylogenetic clusters (Fig. 6), at least based on the partial sequences and the limited sequence data obtained in the current study (e.g. the NS4 cluster included phylotypes from the "WSp" and "SuF samples). Additionally, it has been shown that organisms with very similar 16S rDNA can be very different in their physiological traits [13,44]. The substitution of related, yet ecologically distinct populations over time has been reported previously in bacterioplankton analyses [16,74]. The present study focused on the most abundant *Bacteroidetes* and supported the concept that certain microbial populations become predominant over short periods of time. However, they can be substituted rapidly by related genotypes probably better adapted to the new changing conditions, thus keeping the taxonomic structure rather stable at a family/genus/group level.

Spatial changes of Bacteroidetes assemblages

Previous studies of microbial spatial distribution have commonly reported small changes in bacterioplankton community structure over short superficial transects [11,38,66]. However, some studies have suggested that *Bacteroidetes* diversity at the coast is higher than in the open sea [4,28,48]. In all surface water samples studied here (above a depth of 30 m) spanning a >100 km coast-offshore transect, the contribution of *Bacteroidetes* to total bacterial abundance was uniform and community structure was similar, clustering together in the dendrogram (Fig. 3). An exception was noticed at station MD, in which lower abundance but higher diversity was detected coinciding with an upwelling event in the slope region that was bringing up deep cold water. A similar situation was described by Suzuki et al. [77] in Monterey Bay, where lower percentages of *Bacteroidetes* were observed in the core of an upwelling plume.

Drastic changes in bacterioplankton abundance and community composition usually occur with depth, even across small distances [2,38,51,58,65]. *Bacteroidetes* are usually more abundant in the surface and DCM layers [41,73,82], and the values decrease with depth, usually at a much steeper rate than the bulk bacterial community (Table S1). Our results agreed with these previously reported patterns, showing average surface contributions of approximately 15%, which decreased to 2.5% at 150 m. However, *Bacteroidetes* richness increased with depth even though their abundance decreased (Fig. 1B). Additionally, it was previously described that global bacterioplankton richness increased with depth in the same vertical profiles, suggesting that deeper, probably more stable, ecosystems have a higher bacterial diversity [65].

The analysis of the *Bacteroidetes* community patterns in the spatial transects supported the clustering of two main groups ("Shallow" and "Deep") (Fig. 3) with different phylotypes dominating in each one, although, again, these phylotypes were not phylogenetically different (Fig. 6). Some data from *Bacteroidetes*-specific DGGEs and gene libraries have led to the hypothesis of a

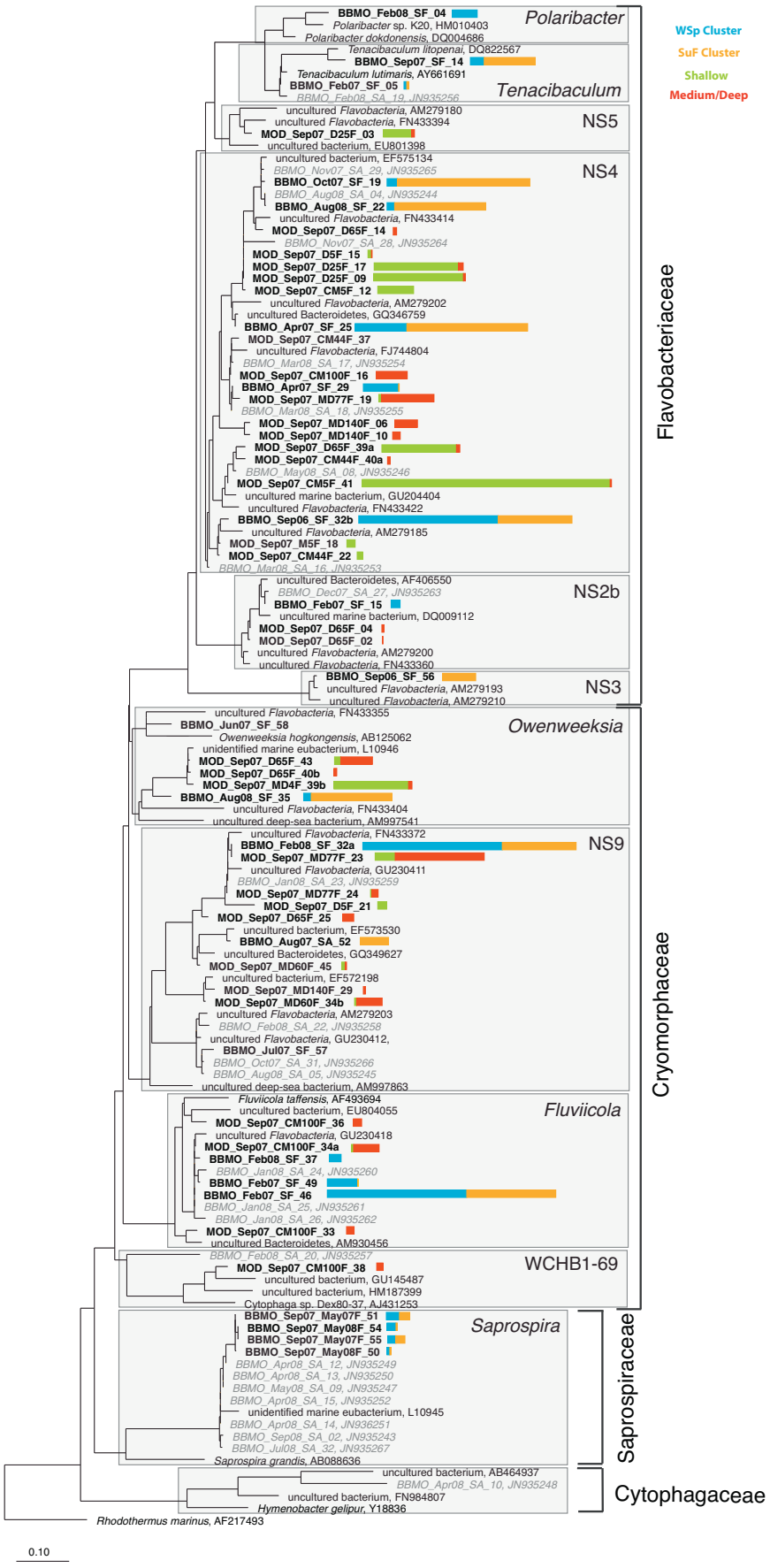

putative depth-specific distribution for the group [14]. However, the current evidence is not enough to clearly resolve the existence of stratified, depth-specific *Bacteroidetes* clades and more detailed studies using high sequencing coverage will be necessary to solve this issue.

Influence of environmental factors

Day length and total bacteria abundance explained a very large variability of *Bacteroidetes* contribution to community structure in the temporal series. Day length has been considered an important variable affecting bacterial diversity in coastal temperate waters [39]. In the particular case of *Bacteroidetes*, this correlation with day length could be attributed to the higher resistance of these organisms to solar radiation compared to other bacterioplankton groups [5,71], or to the presence of proteorhodopsins in a relatively large fraction of marine *Bacteroidetes* for which genomic data are available [34]. Alternatively, the observed correlation could be attributed to additional, unidentified factors covarying with day length.

In the spatial transect, salinity was the best predictor of the *Bacteroidetes* contribution to community structure. *Bacteroidetes* abundance has been negatively correlated with salinity in other studies, since they became less abundant in deep waters [82]. Moreover, they are relatively scarce in recently upwelled waters but their abundance increases as the water ages, and the phytoplankton blooms and decays [77].

Although other authors have found associations between *Bacteroidetes* abundance and algal blooms [12,19,47], we did not find a relationship between Chl *a* concentration and the *Bacteroidetes* percentages. The response of *Bacteroidetes* to the blooms can occur coinciding with the Chl *a* peak or during the detrital phase of the bloom [3]. This may depend on the composition of the blooms [33] but it has also been shown that different *Bacteroidetes* genera may display different responses [79]. Our samples showed maximal abundances one or two months after the Chl *a* peaks, which could indicate a delayed response to the bloom. However, shifts in abundance and composition during blooms may also occur in the order of a few days [33]. In this sense, our monthly samplings would certainly have overlooked this direct effect and any short-term fluctuations.

Interestingly, a positive correlation with temperature was observed in the spatial transects ($r = 0.560$, $p < 0.05$, $n = 17$), even when the analysis included only surface (less than 30 m) water samples ($r = 0.881$, $p < 0.01$, $n = 8$). This contrasts with previous reports in which *Bacteroidetes* abundance correlated negatively with surface temperature [1,41]. Focusing on the taxonomic data obtained in this study, genotypes were identified from the genera *Fluviicola* and *Owenweeksia*, which have mesophilic type strains [50,60]. The latter have been found to be abundantly represented in a pyrosequencing approach with the same samples used in this study [21], and are considered typical Mediterranean species. Moreover, a *Polaribacter* genotype related to an isolate from the Northwestern Mediterranean Sea (*Polaribacter* sp. strain MED152) was also retrieved [42]. Although *Polaribacter* are usually psychrophilic, several isolates have been found to grow optimally at 25–28 °C [84] and sequences from the Mediterranean might belong to a subgroup of warm-water phylotypes, as was suggested for North Atlantic waters [41]. The presence of these mesophilic phylotypes may partly explain the positive correlation with temperature.

Bacteroidetes is one of the most diverse groups in phylogenetic studies of natural environments [49]. An overall similarity of 90.9% was found among all our *Flavobacteria* and *Sphingobacteria* sequences, indicating highly divergent phylotypes. Some values lower than this have also been reported, with *Bacteroidetes* sequences showing 84.9% similarity, whereas *Alphaproteobacteria* sequences had 99.2% similarity, on average, in the Delaware River [49].

Conclusions

The study of *Bacteroidetes* dynamics at a temporal scale during two consecutive years displayed specific phylotypes, detected for Winter-Spring and Summer-Fall, following a recurrent seasonality. Similarly, the *Bacteroidetes* community structure changed with depth but, interestingly, *Bacteroidetes* exhibited its highest diversity in the deepest waters where the abundance was lowest. Furthermore, different physical and biological factors responsible for the changes in the *Bacteroidetes* contributions to total abundance of bacterioplankton were indicated. These factors were markedly different over a temporal series than across a surface-deep gradient. This could be due simply to different environmental conditions that varied differently across each gradient (e.g. day length did not affect communities in surface-depth gradients). As currently defined [53], the phylum *Bacteroidetes* seems highly diverse genetically, and narrower phylogenetic levels within this group would be necessary to identify meaningful units (subgroups, clades or ecotypes) for conducting further detailed ecological studies.

Acknowledgements

We thank Prof. C. Pedrós-Alió and Dr. O. Palenzuela for valuable suggestions and critical reading of the manuscript. B. Díez, V. Balagué, C. Cardelús and I. Forn for DGGE training, and sampling and DNA preparation of the BBMO time series, M. Coll for sampling during the Modivus cruise, and T. Lefort for the flow cytometry data. CDV was a recipient of a JAE-predoc fellowship from CSIC. SGA was supported by a Ramon y Cajal contract from the Spanish Ministry of Science and Innovation and by MicroB3 (FP7-OCEAN-2011). This research was supported by the grants MICRODIVERSITY (CGL2008-00762/BOS), PANGENOMICS (CGL2011-26848/BOS), GEMMA (CTM2007-63753-C02-01/MAR), SUMMER (CTM2008-03309/MAR) and STORM (CTM2009-09352/MAR) from the Spanish Ministry of Science and Innovation (MICINN).

Appendix A. Supplementary data

Supplementary data associated with this article can be found, in the online version, at http://dx.doi.org/10.1016/j.syapm.2013.08.006.

References

[1] Abell, G.C.J., Bowman, J.P. (2005) Colonization and community dynamics of class Flavobacteria on diatom detritus in experimental mesocosms based on Southern Ocean seawater. FEMS Microbiol. Ecol. 53, 379–391.

Fig. 6. Phylogenetic analysis of the 55 partial 16S rRNA gene sequences retrieved from the group-specific *Bacteroidetes* DGGE gels. Twenty-five sequences from a previous study of the "particle-associated" fraction in the same sampling area [25] were also included in the tree (in gray and italic type). Taxonomic groups are outlined in shaded blocks and are defined by representative sequences from public databases (the GenBank accession number is provided). The presence of the phylotypes obtained in this study in each group of samples is represented by a colored horizontal bar displaying the relative contribution of that phylotype (i.e. intensity of the DGGE band as compared to the total band intensity in that type of analysis: WSp/SuF, Shallow/Deep). The scale bar represents 10% of the estimated sequence divergence.

[2] Acinas, S.G., Rodríguez-Valera, F., Pedrós-Alió, C. (1997) Spatial and temporal variation in marine bacterioplankton diversity as shown by RFLP fingerprinting of PCR amplified 16S rDNA. FEMS Microbiol. Ecol. 24, 27–40.

[3] Alderkamp, A.C., Sintes, E., Herndl, G.J. (2006) Abundance and activity of major groups of prokaryotic plankton in the coastal North Sea during spring and summer. Aquatic Microbial Ecology 45, 237–246.

[4] Alonso, C., Warnecke, F., Amann, R., Pernthaler, J. (2007) High local and global diversity of Flavobacteria in marine plankton. Environ. Microbiol. 9, 1253–1266.

[5] Alonso-Sáez, L., Gasol, J.M., Lefort, T., Hofer, J., Sommaruga, R. (2006) Effect of natural sunlight on bacterial activity and differential sensitivity of natural bacterioplankton groups in northwestern Mediterranean coastal waters. Appl. Environ. Microbiol. 72, 5806–5813.

[7] Alonso-Sáez, L., Vázquez-Domínguez, E., Cardelús, C., Pinhassi, J., Sala, M., Lekunberri, I., Balagué, V., Vila-Costa, M., Unrein, F., Massana, R., Simó, R., Gasol, J.M. (2008) Factors controlling the year-round variability in carbon flux through bacteria in a coastal marine system. Ecosystems 11, 397–409.

[8] Altschul, S.F., Gish, W., Miller, W., Myers, E.W., Lipman, D.J. (1990) Basic local alignment search tool (BLAST). J. Mol. Biol. 215, 403–410.

[9] Amann, R.I., Fuchs, B.M. (2008) Single cell identification in microbial communities by improved fluorescence in situ hybridization techniques. Nat. Rev. Microbiol. 6, 339–348.

[11] Bano, N., Hollibaugh, J.T. (2002) Phylogenetic composition of bacterioplankton assemblages from the Arctic Ocean. Appl. Environ. Microbiol. 68, 505–518.

[12] Bauer, M., Kube, M., Teeling, H., Richter, M., Lombardot, T., Allers, E., Würdemann, C.A., Quast, C., Kuhl, H., Knaust, F., Woebken, D., Bischof, K., Mussmann, M., Choudhuri, J.V., Meyer, F., Reinhardt, R., Amann, R., Glöckner, F.O. (2006) Whole genome analysis of the marine Bacteroidetes '*Gramella forsetii*' reveals adaptations to degradation of polymeric organic matter. Environ. Microbiol. 8, 2201–2213.

[13] Béjà, O., Koonin, E.V., Aravind, L., Taylor, L.T., Seitz, H., Stein, J.L., Bensen, D.C., Feldman, R.A., Swanson, R.V., Delong, E.F. (2002) Comparative genomic analysis of archaeal genotypic variants in a single population and in two different oceanic provinces. Appl. Environ. Microbiol. 68, 335–345.

[14] Blümel, M., Süling, J., Imhoff, J.F. (2007) Depth-specific distribution of Bacteroidetes in the oligotrophic eastern Mediterranean Sea. Aquat. Microb. Ecol. 46, 209–224.

[15] Brinkmeyer, R., Knittel, K., Jürgens, J., Weyland, H., Amann, R., Helmke, E. (2003) Diversity and structure of bacterial communities in Arctic versus Antarctic pack ice. Appl. Environ. Microbiol. 69, 6610–6619.

[16] Casamayor, E.O., Pedrós-Alió, C., Muyzer, G., Amann, R. (2002) Microheterogeneity in 16S ribosomal DNA-defined bacterial populations from a stratified planktonic environment is related to temporal changes and to ecological adaptations. Appl. Environ. Microbiol. 68, 1706–1714.

[17] Chen, X., Zeng, Y., Jiao, N. (2006) Development and evaluation of specific 16S rDNA primers for marine Cytophaga–Flavobacteria cluster. Mol. Ecol. Notes 6, 1278–1281.

[18] Cottrell, M., Kirchman, D. (2000) Community composition of marine bacterioplankton determined by 16S rRNA gene clone libraries and fluorescence in situ hybridization. Appl. Environ. Microbiol. 66, 5116–5122.

[19] Cottrell, M., Kirchman, D. (2000) Natural assemblages of marine proteobacteria and members of the Cytophaga–Flavobacter cluster consuming low- and high-molecular weight dissolved organic matter. Appl. Environ. Microbiol. 66, 1692–1697.

[21] Crespo, B.G., Pommier, T., Fernández-Gómez, B., Pedrós-Alió, C. (2013) Taxonomic composition of the particle attached and free-living bacterial assemblages in the Northwest Mediterranean Sea analyzed by pyrosequencing of the 16S rRNA. Microbiology Open 2, 541–552.

[22] Crump, B.C., Armbrust, E.V., Baross, J.A. (1999) Phylogenetic analysis of particle-attached and free-living bacterial communities in the Columbia River, its estuary, and the adjacent coastal ocean. Appl. Environ. Microbiol. 65, 3192–3204.

[23] De Gregoris, T.B., Aldred, N., Clare, A.S., Burgess, J.G. (2011) Improvement of phylum- and class-specific primers for real-time PCR quantification of bacterial taxa. J. Microbiol. Methods 86, 351–356.

[24] Delong, E.F., Franks, D.G., Alldredge, A.L. (1993) Phylogenetic diversity of aggregate-attached vs. free-living marine bacterial assemblages. Limnol. Oceanogr. 38, 924–934.

[25] Díez-Vives, C., Gasol, J.M., Acinas, S.G. (2012) Evaluation of marine Bacteroidetes-specific primers for microbial diversity and dynamics studies. Microb. Ecol. 64, 1047–1055.

[26] Doval, M.D., Álvarez-Salgado, X.A., Gasol, J.M., Lorenzo, L.M., Mirón, I., Figueiras, F.G., Pedrós-Alió, C. (2001) Dissolved and suspended organic carbon in the Atlantic sector of the Southern Ocean, Stock dynamics in upper ocean waters. Mar. Ecol. Prog. Ser. 223, 27–38.

[27] Eilers, H., Pernthaler, J., Glockner, F., Amann, R. (2000) Culturability and in situ abundance of pelagic bacteria from the North Sea. Appl. Environ. Microbiol. 66, 3044–3051.

[28] Eilers, H., Pernthaler, J., Peplies, J., Glöckner, F.O., Gerdts, G., Amann, R. (2001) Isolation of novel pelagic bacteria from the German Bight and their seasonal contributions to surface picoplankton. Appl. Environ. Microbiol. 67, 5134–5142.

[29] Estrada, M., Salat, J. (1989) Phytoplankton assemblages of deep and surface water layers in a Mediterranean frontal zone. Sci. Mar. 53, 203–214.

[30] Estrada, M., Marrasé, C., Latasa, M., Berdalet, E. (1993) Variability of deep chlorophyll maximum characteristics in the Northwestern Mediterranean. Mar. Ecol. Prog. Ser. 92, 289–300.

[31] Estrada, M., Varela, R.A., Salat, J., Cruzado, A., Arias, E. (1999) Spatio-temporal variability of the winter phytoplankton distribution across the Catalan and North Balearic fronts (NW Mediterranean). J. Plankton Res. 21, 1–20.

[32] Fandino, L.B., Riemann, L., Steward, G.F., Long, R.A., Azam, F. (2001) Variations in bacterial community structure during a dinoflagellate bloom analyzed by DGGE and 16S rDNA sequencing. Aquat. Microb. Ecol. 23, 119–130.

[33] Fandino, L.B., Riemann, L., Steward, G.F., Azam, F. (2005) Population dynamics of Cytophaga–Flavobacteria during marine phytoplankton blooms analyzed by real-time quantitative PCR. Aquat. Microb. Ecol. 40, 251–257.

[34] Fernández-Gómez, B., Richter, M., Schüler, M., Pinhassi, J., Acinas, S.G., González, J.M., Pedrós-Alió, C. (2013) Ecology of marine Bacteroidetes: a comparative genomics approach. ISME J. 7, 1–12.

[35] Gasol, J.M., Del Giorgio, P.A. (2000) Using flow cytometry for counting natural planktonic bacteria and understanding the structure of planktonic bacterial communities. Sci. Mar. 64, 197–224.

[36] Gasol, J.M., Doval, M.D., Pinhassi, J., Calderón-Paz, J.I., Guixa-Boixareu, N., Vaqué, D., Pedrós-Alió, C. (1998) Diel variations in bacterial heterotrophic activity and growth in the northwestern Mediterranean Sea. Mar. Ecol. Prog. Ser. 164, 107–124.

[37] Gasol, J.M., Massana, R., Simó, R., Marrasé, C., Acinas, S.G., Pedrós-Alió, C., Pelejero, C., Sala, M.M., Calvo, E., Vaqué, D., Peters, F. (2012) Blanes Bay (site 55). In: O'Brien, T.D., Li, W.K.W., Morán, X.A.G. (Eds.), ICES Phytoplankton and Microbial Plankton Status Report 2009/2010. ICES Cooperative Research Report No. 313, pp. 138–141, 196 pp.

[38] Ghiglione, J.F., Larcher, M., Lebaron, P. (2005) Spatial and temporal scales of variation in bacterioplankton community structure in the NW Mediterranean Sea. Aquat. Microb. Ecol. 40, 229–240.

[39] Gilbert, J.A., Steele, J.A., Caporaso, J.G., Steinbrück, L., Reeder, J., Temperton, B., Huse, S., McHardy, A.C., Knight, R., Joint, I., Somerfield, P., Fuhrman, J.A., Field, D. (2012) Defining seasonal marine microbial community dynamics. ISME J. 6, 298–308.

[40] Glöckner, F.O., Fuchs, B.M., Amann, R. (1999) Bacterioplankton compositions of lakes and oceans: a first comparison based on fluorescence in situ hybridization. Appl. Environ. Microbiol. 64, 3721–3726.

[41] Gómez-Pereira, P.R., Fuchs, B.M., Alonso, C., Oliver, M.J., van Beusekom, J.E., Amann, R. (2010) Distinct flavobacterial communities in contrasting water masses of the North Atlantic Ocean. ISME J. 4, 472–487.

[42] González, J.M., Fernández-Gómez, B., Fernàndez-Guerra, A., Gomez-Consarnau, L., Sánchez, O., Coll-Lladó, M., del Campo, J., Escudero, L., Rodríguez-Martínez, R., Alonso-Sáez, L., Latasa, M., Paulsen, I., Nedashkovskaya, O., Lekunberri, I., Pinhassi, J., Pedrós-Alió, C. (2008) Genome analysis of the proteorhodopsin-containing marine bacterium *Polaribacter* sp. MED152 (Flavobacteria). Proc. Natl. Acad. Sci. USA 105, 8724–8729.

[43] Guixa-Boixereu, N., Vaqué, D., Gasol, J.M., Pedrós-Alió, C. (1999) Distribution of viruses and their potential effect on bacterioplankton in an oligotrophic marine system. Aquat. Microb. Ecol. 19, 205–213.

[44] Jaspers, E., Overmann, J. (2004) Ecological significance of microdiversity: identical 16S rRNA gene sequences can be found in bacteria with highly divergent genomes and ecophysiologies. Appl. Environ. Microbiol. 70, 4831–4839.

[45] Jaspers, E., Nauhaus, K., Cypionka, H., Overmann, J. (2001) Multitude and temporal variability of ecological niches as indicated by the diversity of cultivated bacterioplankton. FEMS Microbiol. Ecol. 36, 153–164.

[46] Kan, J., Wang, K., Chen, F. (2006) Temporal variation and detection limit of an estuarine bacterioplankton community analyzed by denaturing gradient gel electrophoresis (DGGE). Aquat. Microb. Ecol. 42, 7–18.

[47] Kirchman, D.L. (2002) The ecology of Cytophaga–Flavobacteria in aquatic environments. FEMS Microbiol. Ecol. 39, 91–100.

[48] Kirchman, D.L., Yu, L., Cottrell, M.T. (2003) Diversity and abundance of uncultured Cytophaga-like bacteria in the Delaware Estuary. Appl. Environ. Microbiol. 69, 6587–6596.

[49] Kirchman, D.L., Dittel, A.I., Malmstrom, R.R., Cottrell, M.T. (2005) Biogeography of major bacterial groups in the Delaware Estuary. Limnol. Oceanogr. 50, 1697–1706.

[50] Lau, K.W.K., Ng, C.Y.M., Ren, J., Lau, S.C.L., Qian, P.Y., Wong, P.K., Lau, T.C., Wu, M. (2005) *Owenweeksia hongkongensis* gen. nov., sp. nov., a novel marine bacterium of the phylum 'Bacteroidetes'. Int. J. Syst. Evol. Microbiol. 55, 1051–1057.

[51] Lee, S., Fuhrman, J.A. (1991) Spatial and temporal variation of natural bacterioplankton assemblages studied by total genomic DNA cross-hybridization. Limnol. Oceanogr. 36, 1277–1287.

[52] Ludwig, W., Strunk, O., Westram, R., Richter, L., Meier, H., Yadhukumar, A., Buchner, T., Lai, S., Steppi, G., Jobb, W., Förster, I., Brettske, S., Gerber, A.W., Ginhart, O., Gross, S., Grumann, S., Hermann, R., Jost, A., König, T., Liss, R., Lüßmann, M., May, B., Nonhoff, B., Reichel, R., Strehlow, A., Stamatakis, N., Stuckmann, A., Vilbig, M., Lenke, T., Ludwig, A., Bode, K.H., Schleifer, (2004) ARB: a software environment for sequence data. Nucleic Acids Res. 32, 1363–1371.

[53] Ludwig, W., Euzéby, J., Whitman, W.B. (2010) Road map of the phyla Bacteroidetes, Spirochaetes, Tenericutes (Mollicutes), Acidobacteria, Fibrobacteres, Fusobacteria, Dictyoglomi, Gemmatimonadetes, Lentisphaerae, Verrucomicrobia, Chlamydiae, and Planctomycetes, in: Krieg, N.R., Staley, J.T., Brown, D.R., Hedlund, B.P., Paster, B.J., Ward, N.L., Ludwig, W., Whitman, W.B. (Eds.), Bergey's Manual of Systematic Bacteriology, vol. 4, 2nd ed., Springer-Verlag, New York, NY, USA, pp. 1–19.

[54] Malmstrom, R.R., Straza, T.R.A., Cottrell, M.T., Kirchman, D.L. (2007) Diversity, abundance, and biomass production of bacterial groups in the western Arctic Ocean. Aquat. Microb. Ecol. 47, 45–55.

[55] Marie, D., Partensky, F., Jacquet, S., Vaulot, D. (1997) Enumeration and cell cycle analysis of natural populations of marine picoplankton by flow cytometry using the nucleic acid stain SYBR Green I. Appl. Environ. Microbiol. 63, 186–193.
[56] Mary, I., Cummings, D.G., Biegala, I.C., Burkill, P.H., Archer, S.D., Zubkov, M.V. (2006) Seasonal dynamics of bacterioplankton community structure at a coastal station in the western English Channel. Aquat. Microb. Ecol. 41, 119–126.
[57] Massana, R., Murray, A.E., Preston, C.M., Delong, E.F. (1997) Vertical distribution and phylogenetic characterization of marine planktonic Archaea in the Santa Barbara Channel. Appl. Environ. Microbiol. 63, 50–56.
[58] Moeseneder, M.M., Winter, C., Herndl, G.J. (2001) Horizontal and vertical complexity of attached and free-living bacteria of the eastern Mediterranean Sea, determined by 16S rDNA and 16S rRNA fingerprints. Limnol. Oceanogr. 46, 95–107.
[59] Muyzer, G., Brinkhoff, T.T., Nübel, U., Santegoeds, C., Schäfer, H., Wawer, C. (1998) Denaturing gradient gel electrophoresis (DGGE) in microbial ecology. In: Akkermans, A.D.L., van Elsas, J.D., Bruijn, F.J. (Eds.), Molecular Microbial Ecology Manual, Kluwer, Dordrecht, pp. 3.4.4/1–3.4.4/27.
[60] O'Sullivan, L.A., Fuller, K.E., Thomas, E.M., Turley, C.M., Fry, J.C., Weightman, A.J. (2004) Distribution and culturability of the uncultivated 'AGG58 cluster' of the Bacteroidetes phylum in aquatic environments. FEMS Microbiol. Ecol. 47, 359–370.
[61] Pedrós-Alió, C., Calderón-Paz, J.-I., Guixa-Boixereu, N., Estrada, M., Gasol, J.M. (1999) Bacterioplankton and phytoplankton biomass and production during summer stratification in the northwestern Mediterranean Sea. Deep Sea Res. Part I: Oceanogr. Res. Pap. 46, 985–1019.
[62] Pernthaler, A., Pernthaler, J., Amann, R. (2002) Fluorescence in situ hybridization and catalyzed reporter deposition for the identification of marine bacteria. Appl. Environ. Microbiol. 68, 3094–3101.
[63] Pinhassi, J., Hagström, A. (2000) Seasonal succession in marine bacterioplankton. Aquat. Microb. Ecol. 21, 245–256.
[64] Pinhassi, J., Sala, M.M., Havskum, H., Peters, F., Guadayol, Ò., Malits, A., Marrasé, C. (2004) Changes in bacterioplankton composition under different phytoplankton regimens. Appl. Environ. Microbiol. 70, 6753.
[65] Pommier, T., Neal, P., Gasol, J.M., Coll, M., Acinas, S.G., Pedrós-Alió, C. (2010) Spatial patterns of bacterial richness and evenness in the NW Mediterranean Sea explored by pyrosequencing of the 16S rRNA. Aquat. Microb. Ecol. 61, 221–233.
[66] Riemann, L., Middelboe, M. (2002) Stability of bacterial and viral community compositions in Danish coastal waters as depicted by DNA fingerprinting techniques. Aquat. Microb. Ecol. 27, 219–232.
[67] Riemann, L., Winding, A. (2001) Community dynamics of free-living and particle-associated bacterial assemblages during a freshwater phytoplankton bloom. Microb. Ecol. 42, 274–285.
[68] Riemann, L., Steward, G., Fandino, L., Campbell, L., Landry, M., Azam, F. (1999) Bacterial community composition during two consecutive NE Monsoon periods in the Arabian Sea studied by denaturing gradient gel electrophoresis (DGGE) of rRNA genes. Deep-Sea Res. Part II: Topical Stud Oceanogr. 46, 1791–1811.
[69] Rink, B., Seeberger, S., Martens, T., Duerselen, C.-D., Simon, M., Brinkhoff, T. (2007) Effects of phytoplankton bloom in a coastal ecosystem on the composition of bacterial communities. Aquat. Microb. Ecol. 48, 47–60.
[70] Rink, B., Martens, T., Fischer, D., Lemke, A., Grossart, H.-P., Simon, M., Brinkhoff, T. (2008) Short-term dynamics of bacterial communities in a tidally affected coastal ecosystem. FEMS Microbiol. Ecol. 66, 306–319.
[71] Ruiz-González, C., Lefort, T., Galí, M., Montserrat Sala, M., Sommaruga, R., Simó, R., Gasol, J.M. (2011) Seasonal patterns in the sunlight sensitivity of bacterioplankton from Mediterranean surface coastal waters. FEMS Microbiol. Ecol. 79, 661–674.
[72] Salat, J. (1996) Review of hydrographic environmental factors that may influence anchovy habitats in northwestern Mediterranean. Sci. Mar. 60, 21–32.
[73] Schattenhofer, M., Fuchs, B.M., Amann, R., Zubkov, M.V., Tarran, G.A., Pernthaler, J. (2009) Latitudinal distribution of prokaryotic picoplankton populations in the Atlantic Ocean. Environ. Microbiol. 11, 2078–2093.
[74] Schauer, M., Balagué, V., Pedrós-Alió, C., Massana, R. (2003) Seasonal changes in the taxonomic composition of bacterioplankton in a coastal oligotrophic system. Aquat. Microb. Ecol. 31, 163–174.
[75] Simon, M., Glöckner, O., Amann, R. (1999) Different community structure and temperature optima of heterotrophic picoplankton in various regions of the Southern Ocean. Aquat. Microb. Ecol. 18, 275–284.
[76] Sokal, R.R., Rohlf, F.J. 1995 Biometry, 3rd ed., W.H. Freeman & Company, New York.
[77] Suzuki, M., Nakagawa, Y., Harayama, S., Yamamoto, S. (2001) Phylogenetic analysis and taxonomic study of marine Cytophaga-like bacteria: proposal for *Tenacibaculum* gen. nov. with *Tenacibaculum maritimum* comb. nov. and *Tenacibaculum ovolyticum* comb. nov., and description of *Tenacibaculum mesophilum* sp. nov. and *Tenacibaculum amylolyticum* sp. nov. Int. J. Syst. Evol. Microbiol. 51, 1639–1652.
[78] Tamura, K., Peterson, D., Peterson, N., Stecher, G., Nei, M., Kumar, S. (2011) MEGA5: molecular evolutionary genetics analysis using maximum likelihood, evolutionary distance, and maximum parsimony methods. Mol. Biol. Evol. 28, 2731–2739.
[79] Teeling, H., Fuchs, B.M., Becher, D., Klockow, C., Gardebrecht, A., Bennke, C.M., Kassabgy, M., Huang, S., Mann, A.J., Waldmann, J., Weber, M., Klindworth, A., Otto, A., Lange, J., Bernhardt, J., Reinsch, C., Hecker, M., Peplies, J., Bockelmann, F.D., Callies, U., Gerdts, G., Wichels, A., Wiltshire, K.H., Glöckner, F.O., Schweder, T., Amann, R. (2012) Substrate-controlled succession of marine bacterioplankton populations induced by a phytoplankton bloom. Science (New York, NY) 336, 608–611.
[80] Urdea, M.S., Warner, B.D., Running, J.A., Stempien, M., Clyne, J., Horn, T. (1988) A comparison of non-radioisotopic hybridization assay methods using fluorescent, chemiluminescent and enzyme labeled synthetic oligodeoxyribonucleotide probes. Nucleic Acids Res. 16, 4937–4956.
[82] Wells, L.E., Deming, J.W. (2003) Abundance of bacteria, the Cytophaga-Flavobacterium cluster and Archaea in cold oligotrophic waters and nepheloid layers of the Northwest Passage, Canadian Archipelago. Aquat. Microb. Ecol., 1–13.
[83] Worm, J., Gustavson, K., Garde, K., Borch, N.H., Søndergaard, M. (2001) Functional similarity of attached and free-living bacteria during freshwater phytoplankton blooms. Aquat. Microb. Ecol. 25, 103–111.
[84] Yoon, J.H., Kang, S.J., Oh, T.K. (2006) *Polaribacter dokdonensis* sp. nov., isolated from seawater. Int. J. Syst. Evol. Microbiol. 56, 1251–1255.

Supplementary Information

Spatial and temporal variability among marine Bacteroidetes populations in the NW Mediterranean Sea

Cristina Díez-Vives, Josep M. Gasol and Silvia G. Acinas

Table S1. Bacterial abundance in the 2-year time series (left) and in the spatial transects (right) sampled in the study. Total heterotrophic bacteria were enumerated by flow cytometry (column "Bacteria"), while Bacteroidetes relative abundance (column "% CARD-FISH") is expressed as the percentage of cells labelled by CARD-FISH with a Bacteroidetes specific probe, relative to the total DAPI counts. The Bacteroidetes absolute abundance values inferred from these values are also presented (column "Bacteroidetes"). Monthly samples were taken at BBMO from September 2006 to September 2008 and spatial samples belong to the Modivus cruise, in which C, CM, M, MD and D denote the sampled stations along the horizontal transect, followed by the depth at each sampling point ("St-depth").

Temporal (dd-mm-yy)	***Bacteria*** (10^4 cells ml^{-1})	***% CARD-FISH***	**Bacteroidetes** (10^4 cells ml^{-1})	***Spatial (St-depth)***	***Bacteria*** (10^4 cells ml^{-1})	***% CARD-FISH***	**Bacteroidetes** (10^4 cells ml^{-1})
12-09-06	81.97	11.74 ± 4.6	9.62	**C-4**	75.45	10.01 ± 3.95	7.55
10-10-06	92.75	10.27 ± 2.94	9.52	**C-15**	85.22	2.77 ± 1.85	2.36
07-11-06	56.91	12.69 ± 5.25	7.22	**CM-5**	65.68	8.05 ± 2.61	5.29
11-12-06	89.83	10.14 ± 3.28	9.10	**CM-30**	84.81	3.73 ± 1.89	3.16
16-01-07	43.74	12.18 ± 5.43	5.33	**CM-41**	96.16	13.67 ± 3.13	13.15
20-02-07	48.62	10.66 ± 3.75	5.18	**CM-60**	88.77	3.78 ± 2.4	3.36
20-03-07	81.85	8.06 ± 4.82	6.60	**CM-100**	44.39	2.53 ± 1.24	1.12
24-04-07	52.41	19.18 ± 6.5	10.05	**CM-600**	8.97	0.71 ± 2.53	0.06
15-05-07	64.00	17.98 ± 4.94	11.51	**M-5**	38.26	5.3 ± 3.26	2.03
05-06-07	78.94	10.12 ± 5.72	7.99	**M-48**	52.95	3.83 ± 2.74	2.03
03-07-07	96.45	11.29 ± 4.07	10.89	**M-400**	13.25	1.21 ± 2.51	0.16
01-08-07	88.70	11.09 ± 5.05	9.83	**MD-4**	52.97	2.61 ± 1.83	1.38
12-09-07	63.49	11.38 ± 4.42	7.22	**MD-60**	58.08	6.2 ± 1.86	3.60
16-10-07	70.13	11.65 ± 3.08	8.17	**MD-77**	51.29	2.78 ± 2.43	1.43
13-11-07	66.85	10.33 ± 3.67	6.90	**MD-140**	23.55	2.61 ± 1.82	0.61
11-12-07	65.49	11.23 ± 4.64	7.35	**MD-400**	12.18	1.56 ± 3.05	0.19
15-01-08	82.21	9.24 ± 3.02	7.60	**MD-1900**	5.11	0.66 ± 2.69	0.03
12-02-08	48.33	15.64 ± 8.11	7.56	**D-5**	39.29	15.03 ± 3.02	5.90
11-03-08	76.39	12.89 ± 2.66	9.85	**D-25**	49.24	11.12 ± 2.52	5.48
08-04-08	88.48	15.4 ± 3.15	13.62	**D-40**	51.97	9.49 ± 3.00	4.93
07-05-08	57.05	21.98 ± 4.5	12.54	**D-65**	54.92	6.06 ± 3.12	3.33
02-06-08	62.67	16.92 ± 2.67	10.60	**D-500**	9.91	0.6 ± 2.79	0.06
02-07-08	65.93	16.27 ± 5.31	10.73	**D-2000**	4.26	0.87 ± 2.99	0.04
05-08-08	106.11	14.32 ± 1.64	15.19				
02-09-08	73.46	12.74 ± 2.65	9.36				

Table S2 Summary of the multiple regression models (forward procedures) for the temporal series and the spatial transect. The independent contributions of each variable to the prediction of Bacteroidetes abundances after controlling for all other independent variables are presented (β, or standardized regression coefficients). *P*-values are the significance of each predictor variable within the model.

Dependent variable	Predictor variables	Cumulative R^2	β	*P*
Bacteroidetes abundance (Temporal series)	Day Length	0.404	0.567	0.000
	Bacteria	0.528	0.395	0.007
	NH4	0.628	-0.327	0.018
Bcateroidetes abundance (Spatial transects)	Peuk	0.572	0.736	0.000
	Salinity	0.732	-0.410	0.007

Table S3. GenBank accession numbers and taxonomic affiliation of sequences obtained from DGGE bands, according to the Silva classifier system (Ludwig *et al*., 2004), and their closest match in the GenBank database (the % similarity, accession number, and origin of the sequences are listed). Sample names are coded after the sampling location (BBMO), date, depth (S=surface), filter fraction (F= small-fraction) and band ID#.

			Closest neighbor		
Acc. #	**DGGE band name**	**Taxonomic affiliation**	**%**	**Acc. #**	**Origin**
JX865538	BBMO_Feb08_SF_04	*Polaribacter*	100	EU394574	northern Bay of Biscay, pelagic, particle-associated
JX865539	BBMO_Feb07_SF_05	*Tenacibaculum*	100	EU394574	northern Bay of Biscay, pelagic, particle-associated
JX865540	BBMO_Sep07_SF_14	*Tenacibaculum*	98	AB557541	seawater
JX865541	BBMO_Feb07_SF_15	NS2b marine group	99	GU940787	South China Sea
JX865542	BBMO_Feb08_SF_19	NS4 marine group	99	JF692410	coastal urban watershed; Brazil: Jacarepagua
JX865543	BBMO_Aug08_SF_22	NS4 marine group	99	JF692410	coastal urban watershed; Brazil: Jacarepagua
JX865544	BBMO_Apr07_SF_25	NS4 marine group	100	FJ826359	filtered surface sea water at the contrasting non-bloom station in the Yellow Sea
JX865545	BBMO_Apr07_SF_29	NS4 marine group	100	HQ242382	Line P Station P4 depth of 10m
JX865546	BBMO_Feb08_SF_32a*	NS9 marine group	99	HQ242263	Line P Station P4 depth of 10m
JX865547	BBMO_Feb08_SF_32b*	NS4 marine group	99	GU940946	South China Sea
JX865548	BBMO_Aug08_SF_35	*Owenweeksia*	99	DQ473560	NW Mediterranean seawater microcosm
JX865549	BBMO_Feb07_SF_37	*Fluviicola*	99	JN233066	coastal North Carolina surface water,Beaufort Inlet
JX865550	BBMO_Feb07_SF_46	*Fluviicola*	100	JN233066	coastal North Carolina surface water,Beaufort Inlet
JX865551	BBMO_Feb07_SF_49	*Fluviicola*	99	JN233066	coastal North Carolina surface water,Beaufort Inlet
JX865552	BBMO_May08_SF_50	Saprospiraceae	99	FJ406506	mesocosm; Spain: Bay of Blanes
JX865553	BBMO_May07_SF_51	Saprospiraceae	99	FJ406506	mesocosm; Spain: Bay of Blanes
JX865554	BBMO_Aug07_SF_52	NS9 marine group	100	HM747225	Sanggou Bay (Yellow Sea) marine water assemblages between 0.22 and 3 microns"
JX865555	BBMO_May08_SF_54	Saprospiraceae	99	FJ406506	mesocosm; Spain: Bay of Blanes
JX865556	BBMO_May07_SF_55	Saprospiraceae	99	FJ406506	mesocosm; Spain: Bay of Blanes
JX865557	BBMO_Sep06_SF_56	Flavobacteriaceae	99	FJ745043	surface water at the UGA Marine Institute"; USA: Georgia, Sapelo Island
JX865558	BBMO_Jul07_SF_57	NS9 marine group	99	JN233667	coastal North Carolina surface water,Beaufort Inlet
JX865559	BBMO_Jun07_SF_58	*Owenweeksia*	99	FJ745055	surface water at the UGA Marine Institute"; USA: Georgia, Sapelo Island
JX865560	BBMO_Aug07_SF_59	Verrucomicrobia	99	GU940910	South China Sea

(*) Suffixes “a” and “b” denote sequences obtained from bands located at the same position but on different lanes and containing different sequences, thus corresponding to different phylotypes.

Table S4. GenBank accession numbers, and taxonomic affiliation of sequences obtained from DGGE bands according to the Silva classifier system, and their closest match in the GenBank database (the % similarity, accession number, origin, and depth are listed). Band names are coded after the sampling location (MOD), date, sampling station (C, CM, MD, D), depth, filter fraction (F= small-fraction) and band ID#.

			Closest neighbour		
Acc. #	**DGGE band name**	**Taxonomic affiliation**	**%**	**Acc. #**	**Origin; Depth**
JX865561	MOD_Sep07_D65F_02	NS2b marine group	99	HE647151	Pacific Ocean; Ahe atoll; n.s
JX865562	MOD_Sep07_D25F_03	NS5 marine group	99	FN433302	Atlantic Ocean; n.s.
JX865563	MOD_Sep07_D65F_04	NS2b marine group	99	GU940787	South China Sea; n.s.
JX865564	MOD_Sep07_MD140F_06	NS4 marine group	98	FN433303	Atlantic Ocean; n.s
JX865565	MOD_Sep07_D25F_09	NS4 marine group	99	FN435495	Spain;Mallorca Island; surface coastal seawater
JX865566	MOD_Sep07_MD140F_10	NS5 marine group	98	EU804964	250 miles from Panama City; n.s.
JX865567	MOD_Sep07_C5F_12	NS4 marine group	99	GQ916085	USA; west coast of Florida, Eastern Gulf of Mexico; n.s.
JX865568	MOD_Sep07_D65F_14	NS4 marine group	98	FN433303	Atlantic Ocean; n.s.
JX865569	MOD_Sep07_D5F_15	NS4 marine group	99	DQ656199	East China Sea; surface
JX865570	MOD_Sep07_D65F_16	NS4 marine group	99	HQ163249	Canada; British Columbia, Vancouver Island, Saanich Inlet; 100 m
JX865571	MOD_Sep07_D25F_17	NS4 marine group	99	DQ656199	East China Sea; surface
JX865572	MOD_Sep07_M5F_18	NS4 marine group	99	GU940946	South China Sea; n.s.
JX865573	MOD_Sep07_MD140_19	NS4 marine group	99	FN433461	Atlantic Ocean; n.s.
JX865574	MOD_Sep07_D5F_21	NS9 marine group	96	AB355756	western subarctic Pacific; 5 m
JX865575	MOD_Sep07_MD4F_22	NS4 marine group	99	GU061592	South China Sea; 5 m
JX865576	MOD_Sep07_CM60F_23	NS9 marine group	99	HQ242263	North East Pacific; 10 m
JX865577	MOD_Sep07_MD77F_24	NS9 marine group	99	HQ242263	North East Pacific; 10 m
JX865578	MOD_Sep07_D65F_25	NS9 marine group	100	HQ242263	North East Pacific; 10 m
JX865579	MOD_Sep07_MD140F_29	NS9 marine group	98	GQ915983	USA; west coast of Florida, Eastern Gulf of Mexico; n.s.
JX865580	MOD_Sep07_CM100F_33	*Fluviicola*	99	HQ673135	Northeast subarctic Pacific Ocean; 1000 m
JX865581	MOD_Sep07_CM44F_34a*	*Fluviicola*	100	DQ009095	San Pedro Ocean; 5 m
JX865582	MOD_Sep07_D65F_34b*	NS9 marine group	99	EF572198	Coco's Island site 23 (Costa Rica); n.s.
JX865583	MOD_Sep07_CM100F_36	*Fluviicola*	100	FJ202110	host="Montastraea faveolata; n.s.
JX865584	MOD_Sep07_CM44F_37	NS4 marine group	100	GU940762	South China Sea; n.s.
JX865585	MOD_Sep07_CM100F_38	WCHB1-69	98	HM799100	Puerto Rico Trench; 6000 m
JX865586	MOD_Sep07_MD4F_39a*	NS4 marine group	100	HM117334	Elbo Bay in the NW Meditrranean Sea; surface
JX865587	MOD_Sep07_D65F_39b*	*Owenweeksia*	99	DQ656206	East China Sea; surface
JX865588	MOD_Sep07_CM44F_40a*	NS4 marine group	98	HM117334	Elbo Bay in the NW Meditrranean Sea; surface
JX865589	MOD_Sep07_D65F_40b*	*Owenweeksia*	99	GQ348808	Saanich Inlet; 10 m
JX865590	MOD_Sep07_CM5F_41	NS4 marine group	99	HQ242031	North East Pacific; 10 m
JX865591	MOD_Sep07_D65F_43	*Owenweeksia*	99	GQ348808	Saanich Inlet; 10 m
JX865592	MOD_Sep07_MD60F_45	NS9 marine group	100	GQ915956	USA: west coast of Florida, Eastern Gulf of Mexico; n.s.

(*) Suffixes “a” and “b” denote sequences obtained from bands located at the same position over different lanes but containing different sequences and thus corresponding to different phylotypes.

(n.s) Not specified

Table S5. Percentage similarity of partial 16S rDNA sequences from the Bacteroidetes clusters identified in the DGGE study in the Northwestern Mediterranean Sea. Average similarities of pairwise comparisons within (in boxes) and between groups were estimated from an alignment of 54 sequences using MEGA4 software. The overall similarity (average pairwise percentage similarity of all the sequences retrieved in the study) was 90.97%.

Overall	**Similarity (%)**						
Bacteroidetes Clusters	**NS2b**	**NS4**	**NS9**	***Fluviic.***	***Owen.***	***Polar.***	***Sapros.***
NS2b	99.45						
NS4	94.65	97.04					
Ns9	89.52	89.64	93.87				
Fluviicola	88.73	88.95	89.65	97.47			
Owenweeksia	90.15	90.24	92.36	90.25	96.40		
Polaribacter	91.71	92.15	88.29	88.29	87.87	97.80	
Saprospira	85.12	86.19	86.81	86.81	85.04	83.97	99.45

Figure S1. Bathymetric map of the NW Mediterranean area showing the Blanes Bay Microbial Observatory (BBMO), and the sampling stations of the spatial transect sampled in the MODIVUS cruise (C, CM, M, MD and D). Sampling depth is noted between brackets at each point.

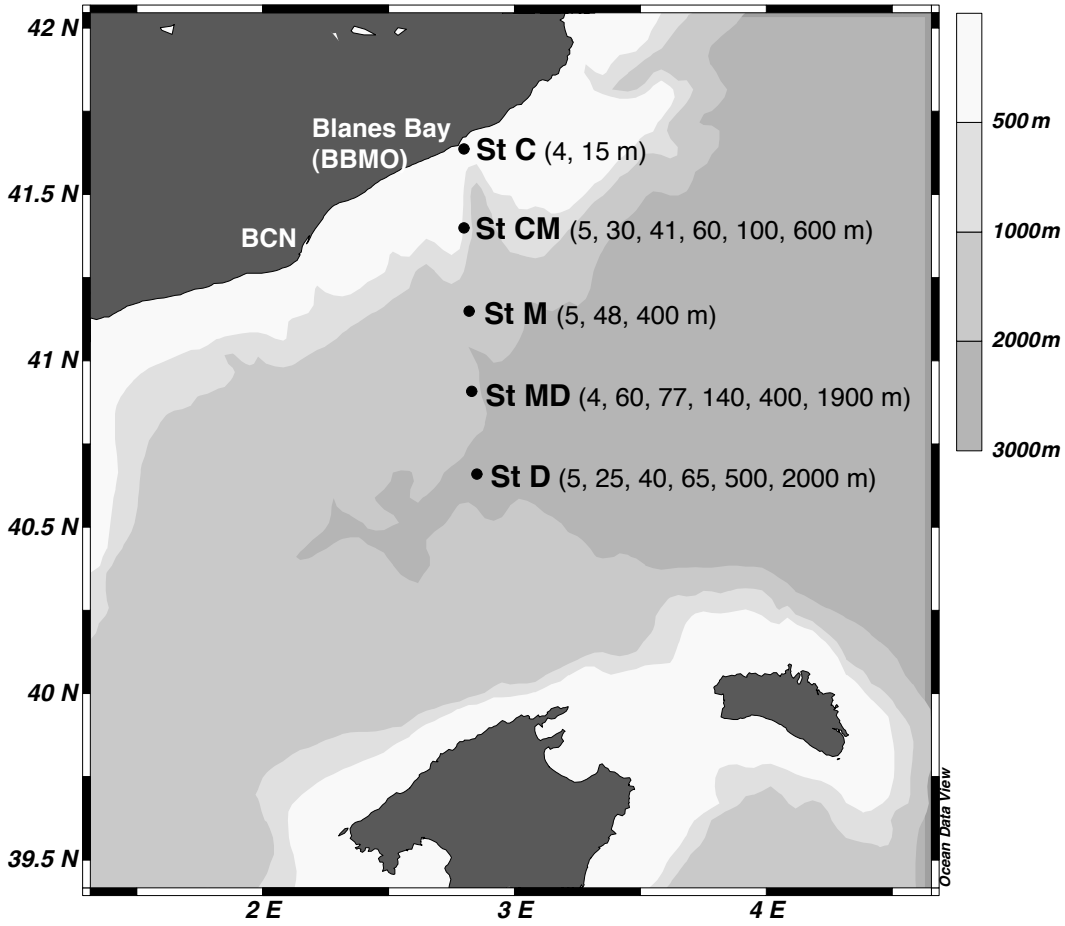

Figure S2. A) Monthly measurements of selected parameters taken during the period September 2006–September 2008, including the division of "Winter-Spring" and "Summer-Fall" groups based on the clustering analyses (see main text). B) Vertical profiles of the same parameters measured at the five stations sampled during the Modivus cruise, including a distinction of surface, DCM, Mesopelagic and Bathypelagic zones.

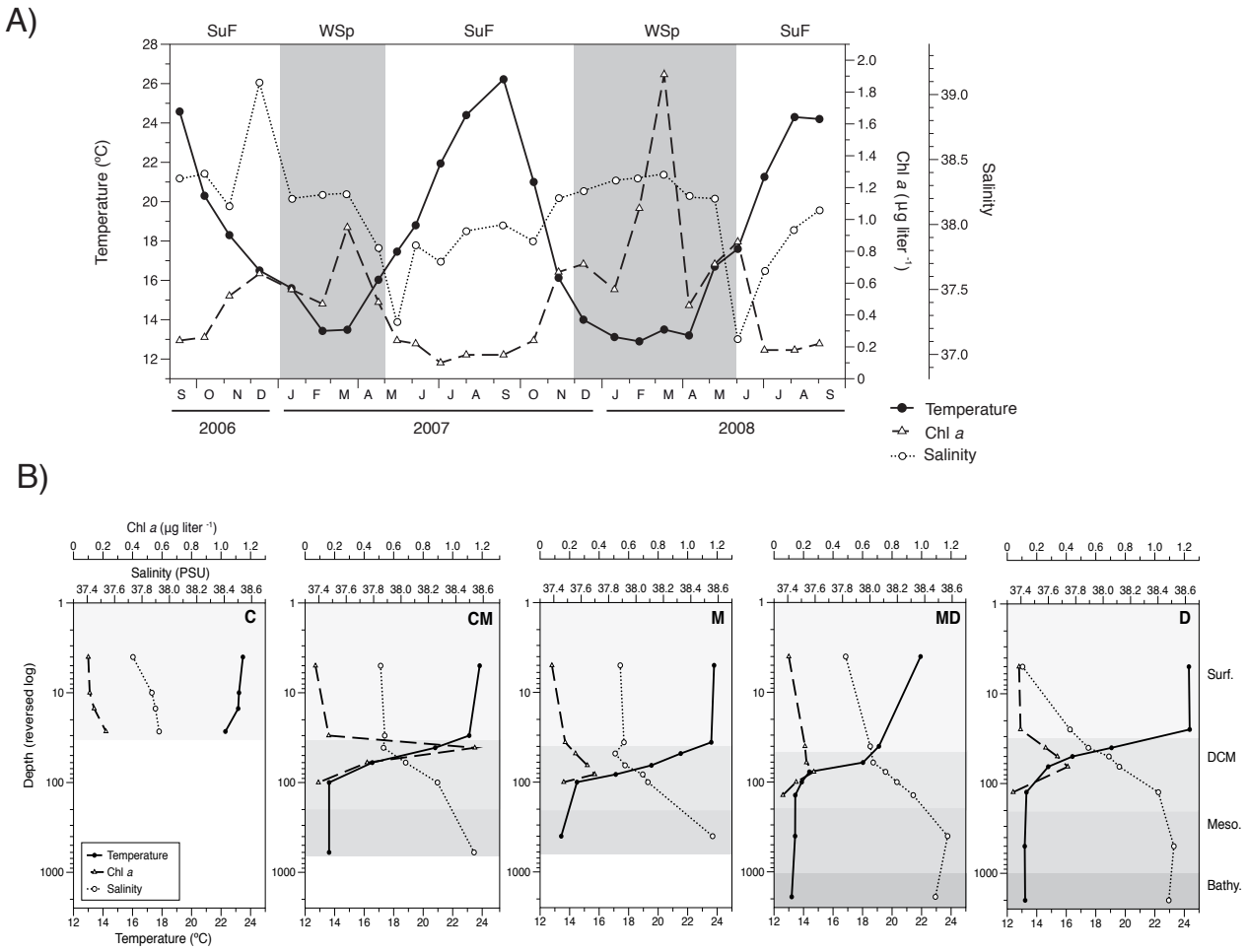

Fig. S3 DGGE analysis of 16S rDNA amplicons using Bacteroidetes-specific primers. Monthly samples over two consecutive years at the coastal sampling point (BBMO). Numbered dots mark the bands that were further excised and sequenced (Table S3). Std standard containing DNA from three marine Bacteroidetes isolates: *Dokdonia* sp. MED134 (DQ481462), *Polaribacter* sp. MED 568 (EU253599), and *Maribacter* sp. MED381 (EU253579)**.**

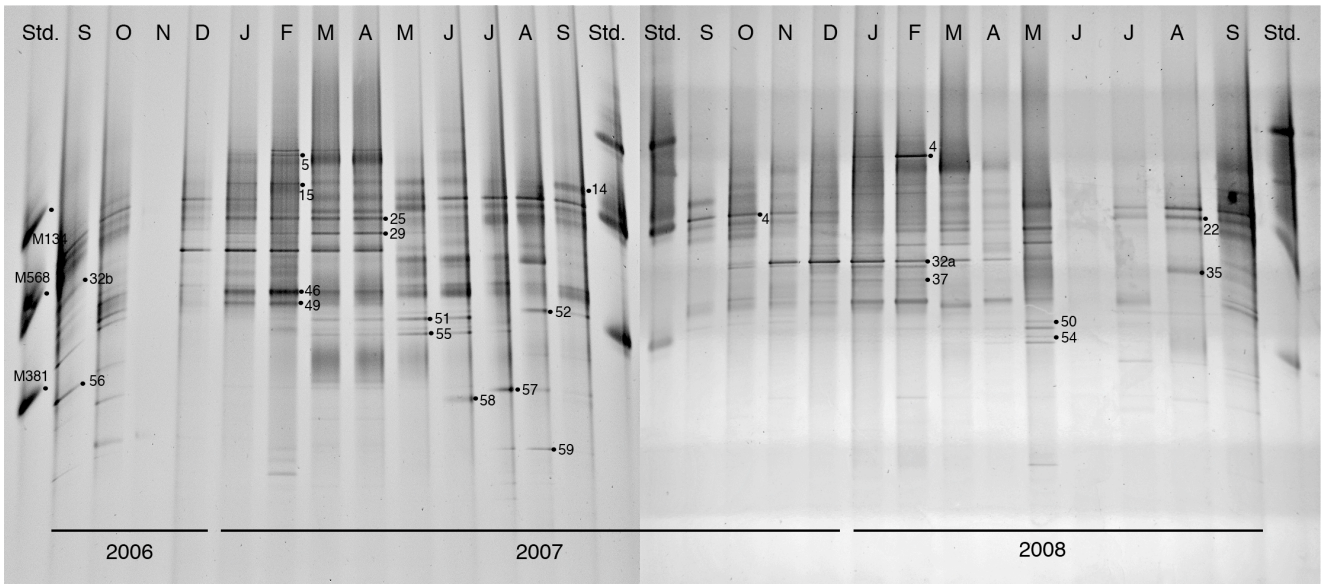

Fig. S4 DGGE analysis of 16S rDNA amplicons using Bacteroidetes-specific primers. The lanes correspond to the different horizontal stations and vertical profiles sampled during the Modivus cruise. Numbered dots mark bands which were further excised and sequenced (Table S4). Std: standards containing DNA from four marine Bacteroidetes isolates: *Dokdonia* sp. MED134 (DQ481462), *Leeuwenhoekiella blandensis* MED217 (DQ294291), *Polaribacter* sp. MED568 (EU253599), and *Maribacter* sp. MED381 (EU253579).

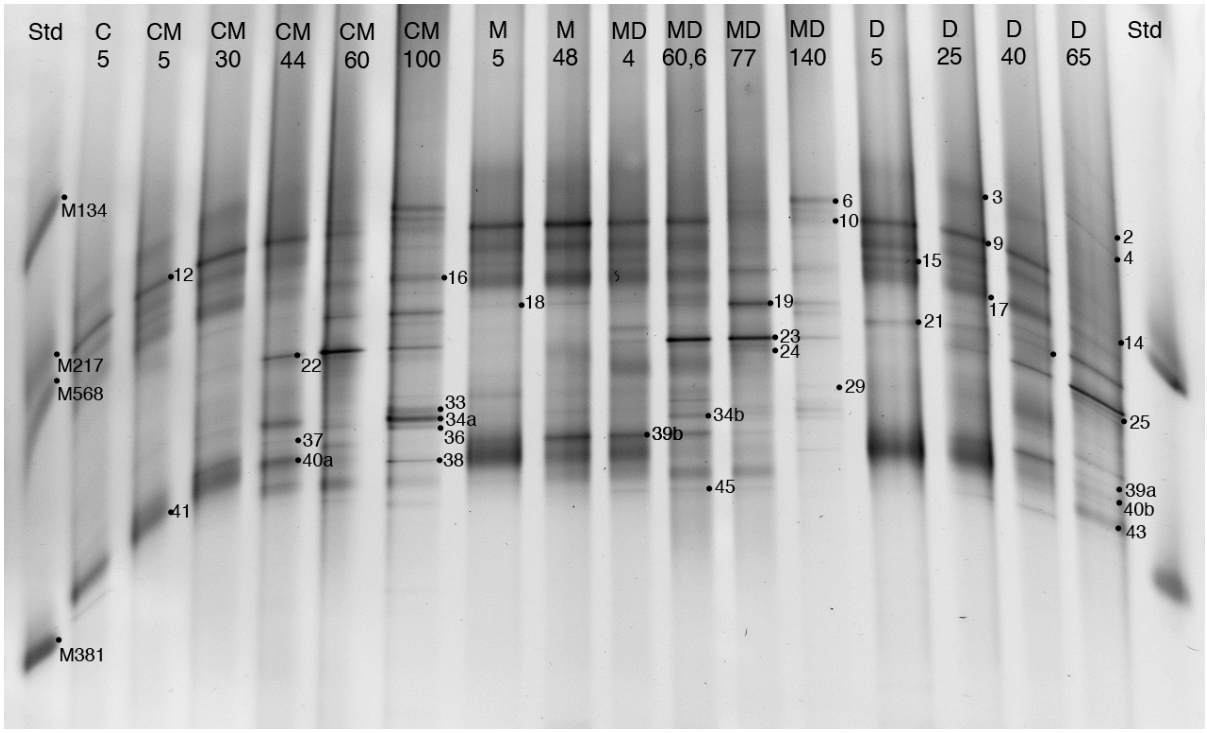

Figure S5. A) DGGE analysis of 16S rDNA amplicons using Universal Bacterial primers. The lanes contain monthly samples over a 1-year time series at the coastal sampling point (BBMO). B) Dendrograms generated from the analysis of DGGE band fingerprints using Bacterial primers (left) and Bacteroidetes-specific primers (right). The distance matrix was calculated using the Bray-Curtis similarity algorithm. The statistical significance of the clustering was calculated using the "similarity profile" permutation tests with Primer 6 software. Samples connected by dashed lines are not significantly different. The arrow marks a difference between both dendrograms in the clustering of samples Dec07 and Jan08. Months that could not be included in the Bacteroidetes study are framed in boxes in the Bacteria dendrogram.